



# Metal-based nanowires in electrical biosensing

Shen-Jie Zhong, Kang-Yu Chen, Shao-Lei Wang, Farid Manshahi,  
Nan Jing, Kai-Dong Wang\*, Shi-Chang Liu\*, Yun-Lei Zhou\* 

Received: 28 January 2024 / Revised: 24 February 2024 / Accepted: 29 February 2024 / Published online: 17 July 2024  
© Youke Publishing Co., Ltd. 2024

**Abstract** Harnessing the unique attributes of metal-based nanowires (MNWs), such as their adaptability, high aspect ratio and conductivity, this review elucidates their burgeoning role as a distinct class of nanomaterials poised to revolutionize sensor technologies. We provide an in-depth examination of MNW assembly methods, highlighting procedural details, foundational principles and performance metrics. Manufacturing electrochemical biosensors and field-effect transistor (FET) biosensors by MNWs offers advantages such as enhanced sensitivity, improved signal-to-noise ratios and increased surface area for efficient biomolecule immobilization. MNWs contribute to precise and reliable biosensing platforms, optimizing the performance of these devices for various applications, such as diagnostics and environmental monitoring.

Electrochemical biosensors are noted for their speed, cost-effectiveness, ease of use and compatibility with compact instrumentation, offering potential for precise biomarker quantification. Meanwhile, FET biosensors demonstrate the potential for early-stage biomarker identification and pharmaceutical applications with nanoscale materials like MNWs, thereby enhancing their detection capabilities. Additionally, we explore the prospects of integrating machine learning and digital health with MNWs in electrical biosensing, charting an innovative path for future advancements in this field. This advancement is facilitated by their electronic properties, compact design and compatibility with existing technologies. We expect this review to highlight future trends and challenges in the use of MNWs for biosensors.

Shen-Jie Zhong and Kang-Yu Chen have contributed equally to this work.

S.-J. Zhong, K.-Y. Chen, Y.-L. Zhou\*  
Hangzhou Institute of Technology, Xidian University, Hangzhou  
311231, China  
e-mail: zhouyunlei@xidian.edu.cn

S.-L. Wang, F. Manshahi, N. Jing  
Department of Bioengineering, Henry Samueli School of  
Engineering and Applied Science, University of California Los  
Angeles, Los Angeles, CA 90095, USA

K.-D. Wang\*  
Division of Cardiology, Department of Medicine, David Geffen  
School of Medicine, University of California Los Angeles, Los  
Angeles, CA 90095, USA  
e-mail: kaidongwang2015@ucla.edu

S.-C. Liu\*  
Hong-Hui Hospital, Xi'an Jiaotong University College of  
Medicine, Xi'an 710054, China  
e-mail: lsc\_2002@outlook.com

**Keywords** Metal-based nanowires; Electrical biosensing;  
Field-effect transistor; Electro-chemical biosensors;  
Machine learning

## 1 Introduction

In the landscape of nanotechnology, metal-based nanowires (MNWs) have emerged as a focal point of academic and research interest [1, 2]. This is attributed to their exceptional properties when compared with their macro-scale counterparts, as documented in numerous scholarly articles [3–7]. The unique characteristics of MNWs, particularly in one-dimensional (1D) electronic density states, can be fine-tuned by manipulating specific parameters [8]. This capability has been especially beneficial in electrochemical applications, where MNWs have been shown to significantly enhance surface area, and consequently,



analytical performance [9–11]. Additionally, the distinctive material structures of MNWs confer them with enhanced electrical conductivity and a larger specific surface area [12–16], thus reducing junction resistance and contributing to their utility in various applications, such as electronics, sensors, photodetectors, energy storage and flexible electronics [17–19].

Recent advancements in the field have highlighted the significant role of MNWs in electrochemical sensing and biosensing [20–24]. A plethora of studies have substantiated the multiple benefits offered by MNWs in these domains [25–27]. Primarily, the extensive surface area of MNWs is instrumental in reducing current densities and overpotentials, thereby greatly improving electrocatalytic efficiency and selectivity in sensing applications [28–30]. Furthermore, this expansive surface area is pivotal in enhancing redox conversions, which significantly boosts analytical sensitivity in both biosensing and electrochemical sensing. This increased sensitivity plays a crucial role in improving the precision and accuracy of these analytical methods. Additionally, the considerable surface area of MNWs enhances reproducibility and provides resistance to fouling, factors that are critical for the long-term stability and reliability of sensing platforms, especially in complex and dynamic environments [31, 32]. Lastly, the unique surface topology of MNWs facilitates improved interactions with biomolecules, a feature of paramount importance in biosensing applications, particularly in complex biological systems where the functionality often hinges on the proximity and interaction of various biomolecules, such as DNA, RNA, proteins, enzymes and cellular components [33–36].

In addition, owing to their unique properties such as high aspect ratios, tunable surface chemistry and excellent electrical conductivity, MNWs have emerged as promising candidates for enhancing field-effect transistor (FET) biosensor performance [37]. Researchers have been actively exploring novel synthesis methods and surface functionalization techniques to tailor MNWs for specific biomolecular interactions. The integration of MNWs into FET biosensors has demonstrated notable advancements in the detection of various biomolecules, such as DNA, proteins and other analytes relevant to biomedical and environmental applications [38, 39]. Studies have focused on optimizing MNWs based FET configurations, refining the immobilization of recognition elements, and improving signal transduction mechanisms. Furthermore, the development of MNWs based FET biosensors has expanded beyond fundamental research to address practical challenges, such as reproducibility, scalability and long-term stability, bringing these sensors closer to real-world applications.

This article aims to explore two primary methodologies employed in the construction of MNW networks: the

bottom-up approach and the top-down approach. The bottom-up approach involves solution-based methods to organize nanowires, which may necessitate additional steps for bonding overlapping wires [40]. In contrast, the top-down approach entails applying a metal layer onto a template or barrier to create a continuous network, thereby effectively eliminating wire-to-wire junction resistance [41, 42]. The integration of MNWs in electrochemical sensing and biosensing capitalizes on their inherent advantages, such as enhanced selectivity, increased sensitivity, improved stability and augmented interaction capabilities with biomolecules. Collectively, these attributes underscore the potential of MNWs as a promising avenue for advancing the efficacy and precision of electrochemical and biosensing technologies.

MNW sensors have shown significant progress in various applications, such as sensing gases, chemicals and biological entities. The ultimate goal of the development of such sensors is to achieve high sensitivity, selectivity and reliability, along with practical considerations such as cost-effectiveness and scalability for mass production. However, there are some key challenges and gaps that existed in the development of MNW sensors [43, 44]. Firstly, enhancing the sensitivity and selectivity of MNW sensors remains a critical goal. Improving the ability of these sensors to detect specific analytes at low concentrations and minimizing interference from other substances is essential. Secondly, long-term stability and durability are important for practical applications. Some MNW may be susceptible to environmental conditions, leading to performance degradation over time. Achieving robust sensors that can withstand extended usage is a challenge. Thirdly, adapting MNW sensors to work effectively in real-world conditions, which may involve complex and variable environments, is a challenge. This includes addressing issues related to humidity, temperature and other external factors that can affect sensor performance. Lastly, developing low-power consumption sensors is important, especially for applications where energy efficiency is a critical factor, such as in wearable devices and remote sensing applications. It's important to note that researchers continue to work towards overcoming these obstacles and pushing the boundaries of what is possible with MNW sensors.

Certainly, the development and use of MNW sensors, like any emerging technology, come with ethical and environmental considerations. The production and synthesis of MNW sensors, may involve the use of energy-intensive processes and chemicals. It's important to assess and minimize the environmental impact associated with the manufacturing and disposal of these materials. Proper disposal of nanomaterials is essential to prevent environmental contamination. Therefore, the rules related to

environmental assessment and recycling pathways need to be specified early to ensure a strategy for responsible disposal or recycling at the end of the MNW equipment life cycle. Previous reviews focus on the application of metal-based materials in a wide range of sensors, or only list the sensing applications of single metal-based materials. This review emphasizes the significance of MNWs in electrical biosensing. As far as we know, no broad review based on MNWs in electrical biosensing has been reported here.

## 2 Synthesis of MNWs

### 2.1 Electrodeposition via template assistance

MNWs can be synthesized using either template-based or template-free methods. Template-based synthesis involves using templates, either hard or soft, to guide the growth of nanowires, allowing for controlled size and shape, ordered arrays and potential for multicomponent structures [45]. Figure 1a presents the template-assisted approach serves as a systematic and efficient means for fabricating MNWs [23, 46, 47]. These templates feature finely-tuned cylindrical pores, which adopt the pore geometry to facilitate

MNWs formation when filled with a chosen material. The critical first step entails choosing a suitable template, with considerations extending to mechanical and chemical resilience, pore geometry, size, and the material of the template. Anodic alumina oxide (AAO) is highly preferred substrate materials for MNWs synthesis [48, 49]. The versatile properties of AAO, such as variable pore sizes, structural strength and thermal stability, make it a prime candidate for template-based electrochemical deposition (Fig. 1b). Their prevalent use in filtration membrane fabrication ensures compatibility with MNWs synthesis. Derived from anodizing pure aluminum films in acidic solutions, alumina templates are highly valued for their homogeneous pore distribution and high pore density [50]. The adaptable nature of the anodization process allows pore diameters to range from a few nanometers to 200 nm. Moreover, alternative porous media, such as porous silicon, zeolites, carbon nanotubes (CNTs), and unique biomolecular structures such as DNA, have also been investigated for their template potential [51, 52]. Although electrochemical deposition is an effective method for the synthesis of metal-based nanowires, there are still some potential challenges in terms of scalability, structural control, and dimensional homogeneity that require in-depth

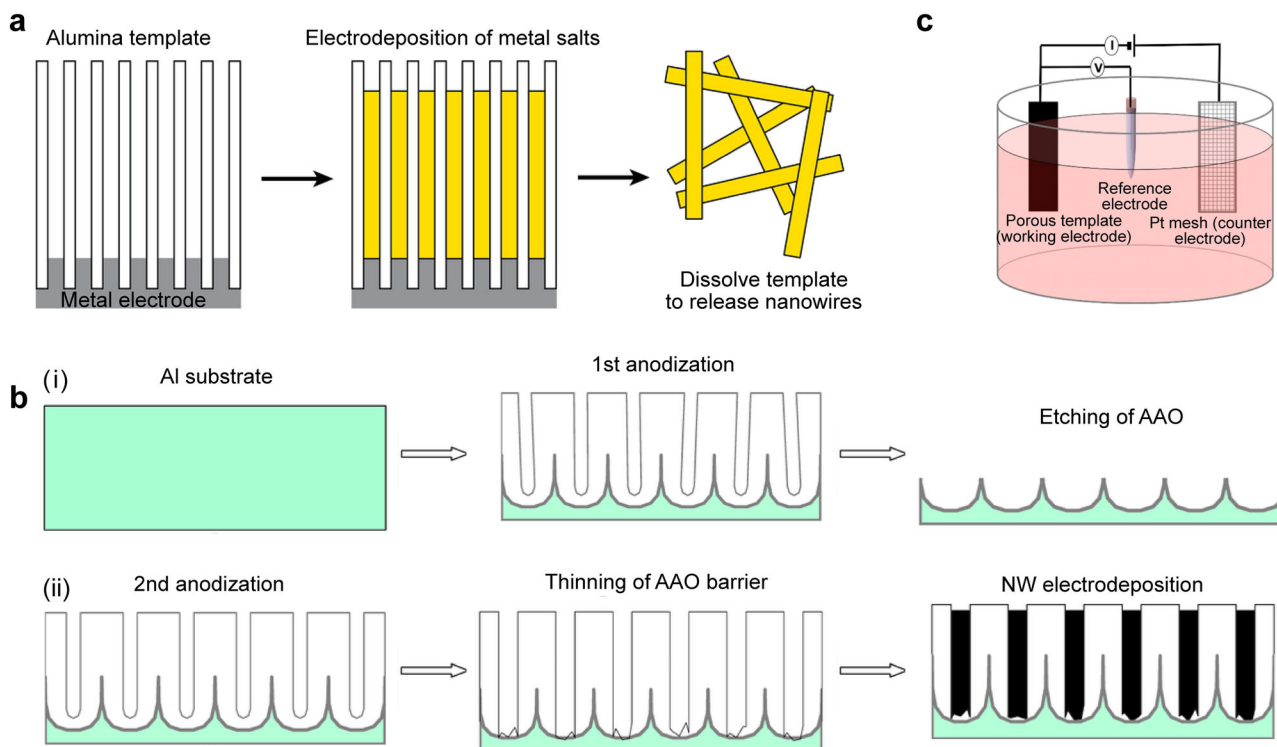


**Fig. 1** Template-assisted synthesis of MNWs. **a** Schematic illustration of electrodeposition of MNWs by a template-assisted method. Reproduced with permission from Ref. [23]. Copyright 2010, WILEY-VCH. **b** Schematic representation of AAO template and steps involved in preparation of NWs. Reproduced with permission from Ref. [48]. Copyright 2016, Elsevier. **c** Schematic illustration of synthesis of magnetic nanowires using a template-assisted electrochemical deposition technique. Reproduced with permission from Ref. [58]. Copyright 2020, Royal Society of Chemistry

research and technology optimization [53]. Firstly, the scalability of electrochemical deposition is an important issue. When preparing metal-based nanowires on a large scale, there is a need to ensure that the process is reproducible and efficient to meet the demands of industrial applications. This may involve optimizing electrochemical deposition conditions and developing automated production processes. Secondly, the structure of the resulting metal-based nanowires may be affected by a number of factors, which is also a key aspect to assess. Factors affecting the structure include the potential of electrodeposition, solution composition, electrode material and experimental conditions. Understanding how these factors affect the morphology, size and crystal structure of nanowires is essential to precisely control and tailor the properties of MNWs [45]. In addition, electrochemical deposition may face challenges related to the inhomogeneity of the nanowire growth rate, which may lead to inhomogeneity in the size distribution [54]. Addressing this issue may involve a better understanding of the relationship between current density and reaction rate, as well as optimizing experimental conditions to ensure uniform growth.

Figure 1c shows the synthesis system typically comprises three electrodes, resembling a standard electrochemical setup [55–59]. An Ag/AgCl electrode serves as the reference electrode, while a platinum wire functions as the counter electrode. After making the electrical contacts, the template is placed at anode and a platinum mesh is used as counter-electrode. The deposition current and voltage are controlled using the reference electrode, where the electric field between the working and counter electrodes forces the free ions to be deposited in the pores. MNWs proliferate upon a distinct substrate designated as the working electrode. Notably, the length of MNWs can be regulated by adjusting the volume of metal deposits through charge control. To maintain the structural and compositional integrity of MNWs, rigorous characterization methods are essential. Conventional geometric parameters, such as length, diameter and chemical composition, are used to define MNWs. Several techniques are employed for verification, with electron microscopy, including transmission electron microscopy (TEM) and scanning electron microscopy (SEM), serving as a cornerstone in the characterization of MNWs [60, 61]. SEM is particularly advantageous due to its versatility in showcasing a diverse array of MNW dimensions and providing a comprehensive perspective on MNWs morphology and surface architecture. Although TEM offers superior magnification, SEM remains the preferred method for visualizing MNWs across a broad size range, spanning from nanometers to micrometers. This approach not only yields a nuanced understanding of MNWs but also enables detailed surface characterization. The significant depth of

field conferred by SEM further permits evaluations of bulk materials [62–64]. Moreover, the capability of SEM to scrutinize large areas proves critical for understanding the spatial distribution of nanomaterials across various surfaces, shedding light on disparities in size distribution. While TEM excels in the high-magnification study of ultra-fine (sub-nanometer) MNWs, field-emission SEM (FESEM) specializes in investigating MNWs distribution on electrode surfaces. FESEM distinguishes itself by capturing high-fidelity images under milder conditions, thus circumventing the need for metallic coatings on the samples [65, 66].

In addition to visual methods, energy-dispersive X-ray spectrometry (EDS) plays a critical role in elemental analysis, offering in-depth insights into MNWs composition and purity [67–70]. X-ray photoelectron spectroscopy (XPS) provides a comprehensive elemental profile, elucidating surface chemical details like empirical formulations and the chemical states of surface-bound entities [71, 72]. When it comes to electrochemical evaluation, cyclic voltammetry (CV) and electrochemical impedance spectroscopy (EIS) are preferred, assisting in comparing electrode behaviors and investigating the complex dynamics at modified electrode interfaces [73, 74].

The process of electrochemical deposition for MNWs hinges on the reduction of metal salts, wherein the required electrons are supplied by an external electrical source, often a potentiostat [75]. The cost-effectiveness of this approach, especially when integrated with membrane methods, has amplified the attractiveness of MNWs. Specifically, the direct template electrodeposition technique relies on the in-pore reduction of metal cations [76]. Upon the application of a potential, these cations migrate through the channels to congregate at the cathode, thereby initiating nanowires (NW) growth within the template. This uncomplicated and budget-friendly technique is typically executed under ambient conditions, obviating the need for specialized equipment. This electrochemical method stands out due to its inherent adaptability, allowing the deposition of a wide array of metals such as Ni, Cu, Au, Zn, Ag, Fe, Pt, Ga, Al and Si [55, 77]. This enables the fabrication of composite MNWs by sequentially depositing different materials, simply by switching the electroplating solution or tweaking the deposition conditions. For example, multi-segmented MNWs of Au and Ni can serve specialized functions like thiol chemistry and magnetic regulation, respectively. An alternative pore-filling approach employs molten metals, where the template is submerged in molten metal, followed by the application of high-pressure gas to ensure complete pore filling.

Template-based synthesis of metal-based nanowires, while offering precise control over size and shape, comes with several limitations and difficulties [78]. The use of

templates, whether hard or soft, introduces complexities and challenges in the preparation process. The fabrication steps involving template preparation and subsequent removal can be intricate and time-consuming, potentially increasing the overall production time and cost [79]. Additionally, the templates themselves may have limitations, such as the need for specialized equipment for their creation. Achieving uniformity in the nanowire arrays can be challenging, as variations in template properties and template removal processes may lead to non-uniform growth. The process may also be sensitive to environmental factors, affecting the reproducibility of the synthesis. Furthermore, in template-based methods, the selection of appropriate templates for specific applications is crucial, and finding templates that are both suitable and easily manipulated can be a challenge [80]. Overall, the limitations in terms of complexity, cost and potential difficulties in achieving uniformity make template-based synthesis of metal-based nanowires a technically demanding process. Researchers continue to address these challenges to enhance the efficiency and scalability of template-based methods for nanowire synthesis.

## 2.2 Electrodeposition via template assistance

Sometimes, template-based methods for preparing MNWs could be complex and involve intricate fabrication processes, adding to production time and cost. In contrast, template-free synthesis relies on spontaneous nucleation and growth without physical templates, offering simplicity, cost-effectiveness and greater flexibility in materials and reaction conditions [81]. While template-free methods may lack the precise control over size and shape seen in template-based approaches, they can yield high-density production and are less constrained by the need for specific templates. The choice between these methods depends on the desired properties for the intended applications, with template-based methods providing precision, and template-free methods offering simplicity and flexibility.

Shifting focus to more streamlined methodologies, researchers have explored simpler alternatives that bypass the complexities associated with template removal (Fig. 2a) [82, 83]. A notable technique employs a metallic wire or electrode as the foundational substrate. By immersing this substrate in a solution containing the necessary reagents and then air-drying, structural quality can be optimized through repeated cycles. Similarly, polymerization of monomers on these electrodes creates surfaces conducive to biomaterial adhesion, such as enzymes, enhancing the electrochemical properties of the resulting electrode.

In template-independent methods, MNWs are fabricated by using nanoparticles (NPs) as the primary building blocks in the steps of Fig. 2b [82, 84]. In a biphasic system containing an aqueous colloidal dispersion of metal-NPs and an organic solvent, such as toluene, intense agitation promotes the transfer of NPs into the organic phase. There, the reduced electrostatic repulsion among NPs encourages aggregation, leading to MNWs formation. The MNWs can be seen as chains of NPs acting as interlinking nodes. This approach eliminates the complex and potentially harmful template extraction step, preserving the integrity of nanostructure.

Chemical vapor deposition (CVD) stands out as a critical technique for the synthesis of carbon nanotubes (CNTs) and is currently under investigation for nanowire manufacturing (Fig. 2c) [85–87]. It involves transforming a vaporized precursor into a solid material on a substrate, such as silicon wafers and metal plates. In the CVD process, the precursor interacts with a heated substrate in a reaction chamber, resulting in solid deposition. While CVD is scalable and has potential for large-scale nanomaterial production, it requires complex equipment, high temperatures and long durations. The method amalgamates a precursor material with a carbon-based reductant, such as graphite powder, within a high-temperature furnace setting. This approach is efficacious for a range of metals, though its efficiency for metal oxides is comparatively diminished due to the stringent conditions required. Compared with gas precursors, which is versatile, CVD for MNWs synthesis has cost advantages. CVD may be more cost-effective and scalable, especially in continuous processes than solvothermal and hydrothermal methods [88]. Polyol synthesis can incur higher costs due to organic solvents, and physical vapor deposition (PVD) may be costlier with vacuum systems [89]. CVD's scalability is often superior to PVD but comparable to other wet-chemical methods. The selection among these template-free methods hinges on factors such as cost, scalability and the specific requirements of nanowire properties for diverse applications.

Adhering to the LaMer paradigm [90], which suggests that nucleation occurs in monodispersed homogenous solutions, the onset of nucleation is triggered at the juncture where the concentration of silver in zero valence state attains a level of supersaturation, as depicted in the second and third steps of Fig. 3a [91]. Subsequent to this phase, commencing at the 120-min mark and persisting until the completion of the synthesis, Ag atoms, which originate from the reduced Ag nitrate, migrate and adhere to the preformed nucleation sites. This migration facilitates the formation of stable metallic linkages amongst the Ag atoms, thereby accelerating the formation of one-dimensional Ag nanostructures. This trajectory is in harmony with foundational concepts in materials science and

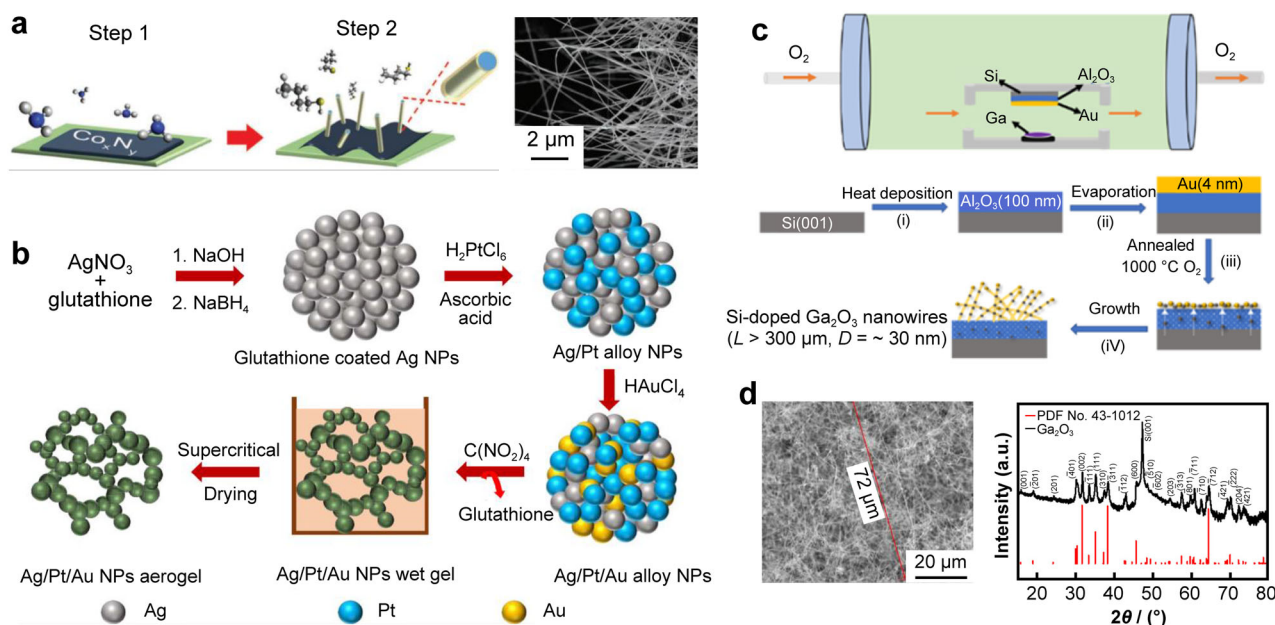


**Fig. 2** Template-free synthesis of MNWs. **a** Schematic illustration of template-free synthesis method. Reproduced with permission from Ref. [82]. Copyright 2016, Royal Society of Chemistry. **b** Schematic illustration of synthesis of glutathione-coated Au/Ag/Pt Alloy NPs via stepwise galvanic replacement reaction of Ag NPs, followed by oxidative self-assembly into monolithic alloy aerogels via removal of surfactant ligands. Reproduced with permission from Ref. [84]. Copyright 2022, American Chemical Society. **c** Schematic diagram of precursors, annealed Al<sub>2</sub>O<sub>3</sub>-film/Si and LPCVD system, and growth process of Ga<sub>2</sub>O<sub>3</sub> NWs. Reproduced with permission from Ref. [87]. Copyright 2023, Multidisciplinary Digital Publishing Institute. **d** SEM image and XRD pattern of Ga<sub>2</sub>O<sub>3</sub> NWs. Reproduced with permission from Ref. [87]. Copyright 2023, Multidisciplinary Digital Publishing Institute

chemistry, yielding insights into the formation of these nanostructures. As conveyed in Fig. 3b, the reduction of the Ag source culminated in the creation of thinner and shorter MNWs [92]. By reducing the concentration of AgNO<sub>3</sub> by 40%, the length of the Ag NWs was markedly reduced, resulting in a broadened length distribution due to the decreased availability of free Ag<sup>+</sup> during the initial stages of MNWs formation. This phenomenon accentuates the profound impact of Ag concentration on the shape of MNWs and dimensions, as portrayed in our empirical data.

Sim et al. [93] manufactured a large-area flexible Organic light-emitting diode (OLED) using a roll-to-roll processing technique (Fig. 3c). Initially, a broad planarized Ag MNWs electrode was constructed on a polyethylene terephthalate (PET) substrate, utilizing a polyimide (PI) film as the substrate to anchor the Ag MNWs. Ag MNWs stabilized using a dispersing agent were deposited onto the PI film via a Meyer rod technique. Following this, a layer of ultraviolet (UV)-reactive prepolymer resin was administered to the surface of the Ag MNWs-coated PI film. This assembly was subsequently laminated with a PET film and subjected to ultraviolet radiation, catalyzing the polymerization of the resin. After curing, the Ag MNWs film encased within the PET film was separated from the PI layer, yielding a transparent electrode [12, 94–97]. This

embedded Ag MNWs electrode offers a planar and smooth surface, obviating the need for an additional planarization stage during OLED construction. These findings substantiate that Ag MNWs, synthesized via the rapid polyol method, emerge as a formidable contender against the brittle indium tin oxide (ITO) in fabricating large-area flexible displays and illumination apparatuses. This pioneering approach showcases potential avenues for scalable and economical manufacturing of next-generation flexible electronics and holds paramount importance in the sphere of progressive materials and device engineering.

The synthesis of bimetallic Cu-Ag nanowires (Cu/Ag MNWs) was achieved via a biphasic approach, initially involving the generation of Cu MNWs, which then underwent a galvanic replacement reaction with Ag, capitalizing on the higher standard reduction potential of Ag (Ag<sup>+</sup> + e<sup>-</sup> → Ag(s), *E* = 0.80 V) relative to Cu (Cu<sup>2+</sup> + 2e<sup>-</sup> → Cu(s), *E* = 0.34 V) (Fig. 3d) [98]. Concurrently, expansive macroscopic two-dimensional (2D) networks of Pt nanowires (Pt MNWs) were intricately crafted through a hierarchical self-assembly process, guided by biomolecular ligands [99–103]. This process initiated with the formation of 1.9 nm-sized nanocrystals, which further assembled into 1D nanowires characterized by a high frequency of grain boundaries (Fig. 3e) [99].

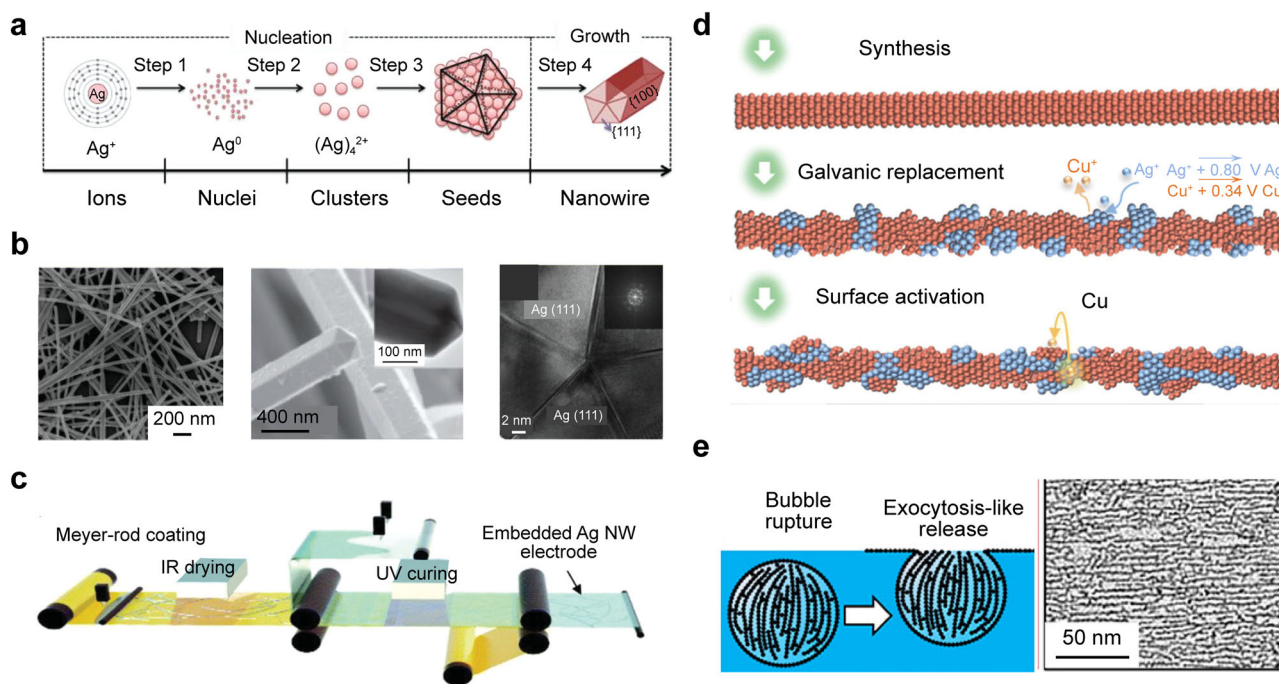


**Fig. 3** Synthesis and assembly processes of MNWs. **a** Schematic diagram of growth mechanism of Ag MNWs. Reproduced with permission from Ref. [95]. Copyright 2015, Elsevier. **b** Electron microscopy snapshots of morphological characteristics of synthesized Ag MNWs. Reproduced with permission from Ref. [96]. Copyright 2016, IOP. **c** Schematic of integration of a Roll-to-Roll system coupled with Meyer rod coating process for efficient material fabrication. Reproduced with permission from Ref. [97]. Copyright 2018, Royal Society of Chemistry. **d** Phases of evolution of Cu MNWs. Reproduced with permission from Ref. [98]. Copyright 2021, Springer. **e** Large-scale hierarchical assembly of an ultrathin Pt MNWs network monolayer at gas/liquid interfaces, enabled by bubble facilitation. Reproduced with permission from Ref. [99]. Copyright 2023, American Chemical Society

These nanowires then interconnected to fabricate extensive monolayer networks extending over centimeter-scale areas. Further investigation into the mechanism revealed that the genesis of these MNWs sheets begins at the gas/liquid interface within synthesis-induced bubbles, with sodium borohydride ( $\text{NaBH}_4$ ) serving as a crucial agent. Upon the disintegration of these bubbles, the Pt MNW sheets are expelled in a manner akin to exocytosis at the gas/liquid boundary, merging to form a contiguous monolayer Pt MNW sheet. The innovative synthesis and the enhanced electrocatalytic attributes of these Pt NWN sheets present substantial potential for various applications, especially within the realm of electrochemical technologies.

### 3 Biosensors fabrications

With miniaturization, fraction of free surfaces increases, which has dominated influence on the total mechanical properties of material.

In developing essential components, researchers employ two predominant strategies, top-down and bottom-up [40, 41, 104, 105]. The top-down approach begins with bulk material and progressively refines it by removing excess portions to achieve the desired configuration, akin to

subtractive manufacturing. This technique is widely used in the electronics industry, especially in semiconductor chip manufacturing, which typically requires photomasks for lithography and chemical or physical etching to realize the intended design [106–108]. Conversely, the bottom-up strategy constructs nano or microarchitectures by sequentially assembling smaller units, similar to building with bricks, where individual atomic or molecular entities interconnect to form the targeted structure. Classic illustrations of bottom-up methodologies encompass chemical synthesis and electrochemical processes, which facilitate the engineering of specific morphological structures.

Inspired by natural architectures, novel procedures have been devised for fabricating micro and nanodevices. For example, natural wooden structures, mussel structures and leaf vein structures. Biological entities such as viruses or proteins serve as templates for nanowire growth, and this bio-template approach utilizes the natural ability of these biomolecules to guide the formation of nanowires with customized structures [109]. Also drawing inspiration from the waterproof properties of lotus leaves, researchers are exploring ways to endow nanowires with hydrophobic properties, which could be valuable in applications such as waterproof coatings and microfluidic devices. Bottom-up strategies provide alternatives to navigate the intrinsic

obstacles presented by top-down approaches, which typically require intricate techniques and advanced instrumentation [105]. Although micro and nano systems have historically relied on top-down fabrication, advancements in small-scale device crafting have broadened the range of techniques [28]. Emulating natural processes, the strategic chemical arrangement of nanoscale materials sets the foundation for the development of devices that exhibit distinctive attributes, which stem from their nanoscopic constituents [110–112]. The advent of novel materials, coupled with the emergence of unanticipated nanoscale phenomena, has been instrumental in forging new frontiers in scientific research.

MNWs are crucial for a bottom-up fabrication approach, enabling the creation of intricate nanostructures and their subsequent assembly for nanotechnological applications [113, 114]. A multitude of techniques such as template-directed electrodeposition, assorted chemical methodologies, and CVD have been explored for the fabrication of MNWs. Among these, template-assisted electrodeposition is notable for its precision in fine-tuning the length, diameter and density by careful adjustment of deposition parameters or the template itself. The ensuing discussion provides an analytical synopsis of these methodologies.

Figure 4a, b illustrates the conceptual differences between bottom-up and top-down methodologies. The top-down approach, while advantageous for achieving precise

alignment and directional control of MNWs, falls short in terms of scalability compared to the bottom-up approach [38]. The ice-templating process has undergone further refinement for the 2D organization of MNWs, resulting in structured and porous networks. Refining the ice-templating process for MNWs involves precise control over freezing conditions, particle dispersion and post-processing steps. Optimization includes temperature gradients, particle size and concentration for uniform ice crystal growth, yielding organized 2D networks [115]. Sequential templating and external fields enhance hierarchical structures and alignment. Controlled sublimation and drying conditions, coupled with densification and sintering, contribute to the final network's mechanical properties. The refined process ensures tailored porosity and spatial arrangement, crucial for applications such as sensors and electronics, in which the specific organization of nanowires influences material performance [116]. A prominent method encompasses the transformation of a three-dimensional (3D) cellular framework into its 2D analog during thawing, leveraging the exceptional malleability of ultra-thin MNWs and the coalescence effects intrinsic to the MNWs. This approach allows for precise control over the mesh dimensions and bundle diameter of the emergent 2D Ag MNWs mesh, optimizing both its photonic and electrical attributes. Freezing from dual-directional sources leads to configurations with perpendicular intersections (Fig. 4c) [117]. The

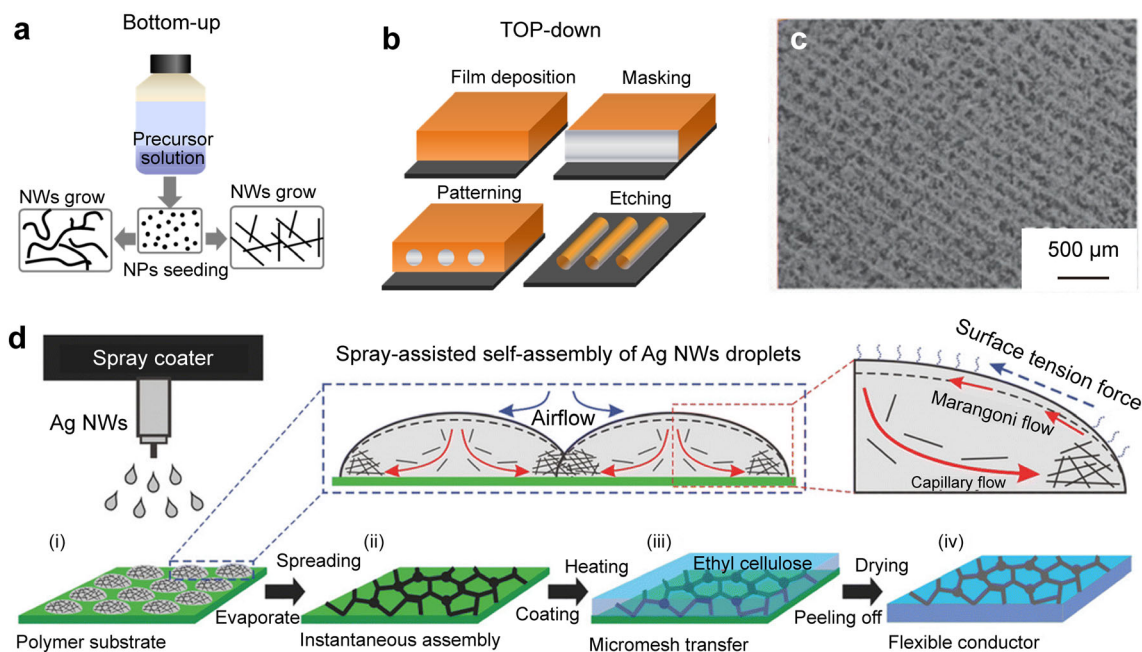


**Fig. 4** Methods for integrating MNWs onto device substrates. **a, b** Depictions of incorporation of MNWs onto substrates utilizing both bottom-up and top-down fabrication methods. Reproduced with permission from Ref. [38]. Copyright 2018, Elsevier. **c** Schematic alongside a corresponding SEM image illustrating perpendicularly arranged Ag NWs designs, conceived through bidimensional ice-guided technique. Reproduced with permission from Ref. [117]. Copyright 2021, WILEY-VCH. **d** Elaboration and underlying principle of construction of Ag NWs microgrid. Reproduced with permission from Ref. [105]. Copyright 2018, WILEY-VCH

deposition pattern of MNWs intricately corresponds to the interplay between capillary and Marangoni flux, with their quantified intensities showcased in Fig. 4d [105]. These dual fluidic mechanisms can be adeptly modulated by calibrating droplet dimensions to the physicochemical characteristics of the ink and substrate. In ice-templating, capillary and Marangoni flux play crucial roles in MNWs deposition [118]. Capillary flux is driven by the pressure difference across the liquid meniscus formed during freezing. As ice grows, liquid is drawn into the solidification front, guiding MNWs alignment. Marangoni flux is influenced by surface tension gradients, causing fluid motion during freezing. Temperature variations lead to differing solute concentrations, inducing surface tension gradients that transport MNWs. Together, these fluidic mechanisms control MNWs positioning, alignment and concentration within the ice template, impacting the final two-dimensional arrangement [119]. Understanding capillary and Marangoni flux is essential for optimizing ice-templating processes and tailoring MNW networks for various applications.

In template-assisted electrodeposition for nanowire synthesis, precision in fine-tuning the length, diameter and density is crucial for tailoring the nanowires to specific applications. Precise control over the applied voltage and deposition time allows researchers to regulate the length of nanowires [120]. Longer deposition time or higher voltages typically result in longer nanowires. The concentration of metal ions in the electrolyte solution and the rate of electrodeposition influence nanowire diameter. Higher ion concentrations and slower deposition rates tend to produce thicker nanowires. The density of nanowires can be tuned by adjusting the template pore size and electrodeposition parameters. Smaller template pores or optimized deposition conditions can lead to higher nanowire densities [121].

## 4 Electrical biosensing

### 4.1 Electrochemical biosensing

The advent of scalable, solution-oriented synthesis methodologies for MNWs has augmented their significance in electrochemical domains [11, 122, 123]. MNWs possess the potential to form cohesive 2D and 3D networks, effectively eliminating the requirement for traditional carbon supports and mitigating the detrimental effects of carbon corrosion. Notably, porous 3D NWs configurations show promise as flow-through electrodes, offering remarkable specific surface areas and superior mass transfer coefficients, which consequently enhance the efficiency of electrochemical sensing (Fig. 5a) [124, 125]. The modifiable surface architecture and dimensions of

MNWs provide researchers with a novel platform to design electrodes ranging from atomic to microscale dimensions, with the primary objective of optimizing electrochemical performance. Currently, MNWs can be synthesized from a diverse spectrum of 23 metals including but not limited to, Ag, Au, Cu, Pd, Pt, Ni and Pb (Fig. 5b) [126, 127]. Among them, Ag excels in high electrical conductivity, cost-effectiveness, and broad applications in electronics [128]. Au offers stability and unique optical properties, advantageous in biomedical sensing and catalysis. The decision balances factors such as cost, electrical performance and specific application needs. For instance, Ag is cost-effective and electrically efficient, while the stability and optical characteristics of Au make it suitable for biomedical and optical applications. The selection hinges on optimizing material properties for targeted functionalities in diverse MNW applications. Recent research trends emphasize Cu-based electrodes due to their advantages in electrochemical reduction processes [129]. Affordability, abundance and excellent conductivity makes Cu an attractive alternative to noble metals [130]. In electrocatalysis, Cu exhibits unique surface reactivity and catalytic activity, particularly in CO<sub>2</sub> reduction reactions. It facilitates selective product formation such as ethylene, thus promoting sustainable energy conversion. Moreover, Cu-based electrodes play a crucial role in advancing green technologies, contributing to the growing interest in renewable energy research and sustainable electrochemical processes, in which properties of Cu offer a balance between cost-effectiveness and performance [131].

Figure 5c shows contrary to the common assumption that surface-to-volume ratio of MNWs is smaller than NPs with analogous diameters, it is essential to highlight that MNWs may exhibit increased specific activity due to their distinct surface morphology [132]. Moreover, the durability of MNWs markedly surpasses that of NPs, an attribute stemming from their resistance to phenomena such as Ostwald ripening, dissolution and detachment from standard carbon backbones [133]. Importantly, MNW arrays can establish highly conductive, standalone frameworks, bypassing reliance on additional carbon supports [134]. These attributes underscore the potential of MNWs to drive innovations in the broader electrochemical sector.

Electrochemical sensors have emerged as a promising avenue to address specific analytical requisites, distinguished by their rapid response, cost-efficiency, operational simplicity and compatibility with miniaturized devices [135–139]. The landscape of electrochemical sensors explored for the quantification of biomarkers is diverse, including impedimetric, chronoamperometric, voltammetric and biosensor modalities [140–143]. Scholars have rigorously assessed an assortment of electrode materials for the detection of biomarkers. Recent research trends have

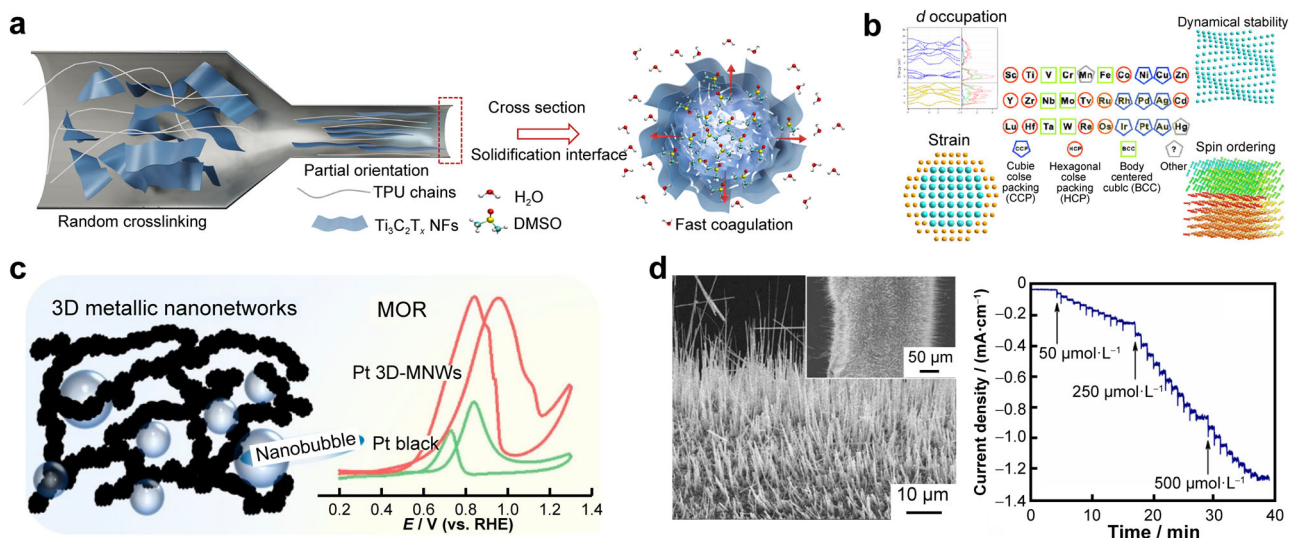


**Fig. 5** MNWs for electrochemical biosensing. **a** Inside diagram and coagulation interface of wet-spinning process for constructing a porous MP hybrid fiber. Reproduced with permission from Ref. [124]. Copyright 2023, American Chemical Society. **b** Crystal phase regulation in noble metal nanocrystals. Reproduced with permission from Ref. [126]. Copyright 2016, American Chemical Society. **c** Electrocatalytic performance of Pt 3D-MNWs tested by methanol oxidation reaction (MOR). Reproduced with permission from Ref. [132]. Copyright 2021, American Chemical Society. **d** Morphology images and structures of Cu wires after electrochemical reduction and amperometric response of Cu MNWs electrode with successive addition of NaNO<sub>3</sub> at -0.46 V. Reproduced with permission from Ref. [144]. Copyright 2018, Elsevier

emphasized Cu-based electrodes, attributable to their inherent electrocatalytic advantages during electrochemical reduction processes. An innovative approach was introduced by Wu et al. [144], wherein a Cu MNWs array was fabricated via the electrochemical reduction of Cu oxide NWs initially generated through thermal oxidation (Fig. 5d). By integrating this electrode with amperometric detection, they adeptly quantified nitrate ions over a linear range of 50 to 600  $\mu\text{mol}\cdot\text{L}^{-1}$ , achieving a detection limit of 12.2  $\mu\text{mol}\cdot\text{L}^{-1}$ . These innovative approaches underscore the progressive strides in the domain of electrochemical sensors enhanced with MNWs.

Patella et al. [145] introduced a nanostructured sensor constituted of an array of Cu MNWs, devised through the galvanic deposition technique (Fig. 6a). These sensors offer an expeditious response time and a remarkable detection limit of less than 10  $\mu\text{mol}\cdot\text{L}^{-1}$  due to their nanoarchitecture. Analytical evaluations under the influence of potential interferents confirmed their negligible impact. Such findings are indicative of groundbreaking strides in devising methods for nitrate ion surveillance. In the synthesis of Cu NWs and Cu MNWs/rGO (reduced graphene oxide) hybrids, ethylenediamine (EDA) stands out as an indispensable structure-directing agent. EDA governs the anisotropic growth of Cu MNWs, stemming from spherical Cu seeds, originating from the reduction of specific Cu complexes, chiefly  $\text{Cu}(\text{OH})_4^{2-}$ , by hydrazine ( $\text{N}_2\text{H}_4$ ) in a highly concentrated alkaline solution. As showcased in Fig. 6b(i), Ju et al. [146] offer SEM images

that delineate the morphology of Cu MNWs. These structures, consistent in their morphology, have a diameter of  $\sim 100$  nm, and their lengths vary from tens to micrometers. High resolution SEM image, highlighted in Fig. 6b(i), presents the pristine surface of the NWs. X-ray diffraction (XRD) pattern of the Cu MNWs/rGO composites is shown in Fig. 6b(ii). A dominant peak at  $23.1^\circ$  corroborates the effective reduction of graphene oxide (GO) to rGO, albeit with some structural disarray. Peaks evident at  $43.3^\circ$ ,  $50.4^\circ$  and  $74.1^\circ$  resonate with the (111), (200) and (311) crystalline planes of Cu, suggesting its face-centered cubic crystal framework (JCPDS No. 04-0836). It is imperative to address the existence of potential interferents, including molecules such as ascorbic acid (AA), dopamine (DA), uric acid (UA) and saccharides such as fructose and sucrose. Thus, the resilience of biosensors against these interferents becomes imperative. This resilience was tested by immersing the sensor in a 0.5  $\text{mmol}\cdot\text{L}^{-1}$  glucose solution, complemented with equal concentrations of potential interferents, as highlighted in Fig. 6b(iii). The resultant electrochemical readings, derived from the oxidation of these compounds, demonstrated minimal interference with glucose oxidation, accentuating the specificity of Cu MNWs/rGO for glucose recognition.

MNWs have carved a niche within the realm of nanomaterials, showcasing significant potential. Their appeal lies in their intrinsic properties: uni-axial conduction pathways, dimensions tailored to the target molecules and

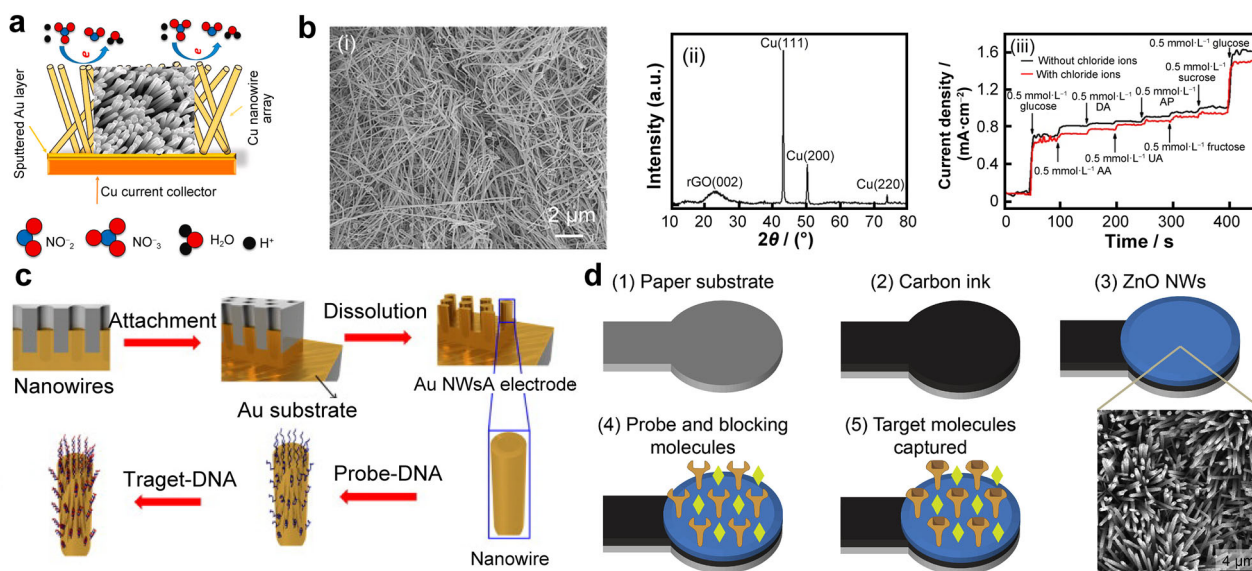


**Fig. 6** Illustrations of various nanowire-based applications. **a** Electrochemical sensor showcasing a Cu MNW array meticulously engineered for selective detection of nitrate ions. Reproduced with permission from Ref. [145]. Copyright 2021, Elsevier. **b** Development of a non-enzymatic amperometric glucose sensor integrating Cu MNWs and rGO layers. Reproduced with permission from Ref. [146]. Copyright 2016, WILEY-VCH. **c** Electrode adaptation employing nanowire complications, bolstering electrochemical discernment capabilities pertinent to nucleic acids. Reproduced with permission from Ref. [147]. Copyright 2013, Elsevier. **d** Amplification of efficacy inherent to paper-based EIS efficacy via ZnO MNWs biosensors. Reproduced with permission from Ref. [148]. Copyright 2021, Elsevier

exemplary electrical transport capability. Illustratively, Au NWs have been employed for detecting Alzheimer's disease detection, GaN NWs in nucleic acid detection (Fig. 6c) [147, 148], TiO<sub>2</sub> MNWs for bacterial monitoring, and Si MNWs for detecting hepatitis B and hepatocellular carcinoma markers, specifically  $\alpha$ -fetoprotein (AFP).

In the domain of EIS, MNWs offer a plethora of designs and orientations, each imparting its unique functional imprint. Although 1D MNWs are integral to semiconducting devices, 3D structures, termed as MNW arrays, are more suitable for multi-component detection systems. The performance efficiency of an MNW array hinges on its fabrication precision, influencing key parameters such as diameter, length, orientation and crystallinity.

Building on this, another exploration detailed the creation of a variety of MNWs of different lengths, anchored on paper matrices. This was achieved using electrodeposition templates, supplemented by efficient adhesive tape-guided patterning conducted at room temperature. Remarkably, this avant-garde strategy revealed an impressive electrode-tissue impedance chart, positioning it as a potential tool for capturing electrocardiographic patterns without the need for conductive gels [149].

To effectively combat infectious disease outbreaks, especially the COVID-19 pandemic, molecular diagnostics that are precise, quick and cost-effective, are indispensable. Microfluidic paper-based analytical devices ( $\mu$ PADs) have risen to prominence as diagnostic instruments

[123, 150–152].  $\mu$ PADs with EIS biosensors offer unique advantages in combating infectious diseases. MNWs enhance EIS biosensor effectiveness by improving electrical conductivity and surface area, enhancing sensitivity for rapid and accurate detection of biomarkers. The integration of MNWs into  $\mu$ PADs facilitates portable, low-cost and point-of-care diagnostics. This amalgamation enables early disease detection, vital for infectious diseases, with the potential for widespread, affordable deployment in resource-limited settings. The synergistic combination of  $\mu$ PADs, EIS biosensors and MNWs underscores a promising approach for accessible and efficient disease diagnostics, supporting global health initiatives. Among diagnostic modalities, EIS biosensors, marked by their label-free approach and increased sensitivity, emerge as vital tools in enhancing diagnostic accuracy. Yet, a notable gap exists in refining EIS biosensing within  $\mu$ PADs. In this context, Li et al. [148] devised an innovative strategy aimed at amplifying the efficacy of EIS biosensors embedded within paper substrates, utilizing ZnO MNWs in-situ grown on working electrodes (WEs) as illustrated in Fig. 6d. By diligently comparing diverse EIS configurations and evaluating the role of ZnO-MNWs in EIS measurements, the team emphasized the efficacy of ZnO-MNW-augmented WEs in supporting Faradaic reactions with iron-based electron mediators. The meticulous calibration of these paper-based EIS biosensors, equipped with various ZnO MNW configurations, resulted in an

impressively low detection limit ( $0.4 \text{ pg}\cdot\text{ml}^{-1}$ ) for identifying a specific antigen, recognized as a biomarker for the human immunodeficiency virus (HIV). Detailed microscopic examination in tandem with electrochemical analysis provided a deeper understanding of the interplay between the structural characteristics of ZnO-MNW-enhanced working electrodes (WEs) and their electrochemical properties, which in turn affect the performances of EIS nanobiosensors and detection capabilities. The investigation further demonstrated the proficiency of these nanobiosensors in detecting assorted concentrations of the IgG antibody (CR3022) against SARS-CoV-2 in human serum samples, with a range extending from nil to  $1 \text{ }\mu\text{g}\cdot\text{ml}^{-1}$ . This study not only reveals a viable approach for crafting superior EIS  $\mu$ PADs but also underscores their potential as rapid diagnostic tools in global health crises.

## 4.2 FET biosensing

FET biosensors have risen to prominence in the sphere of early biomarker identification and pharmaceutical assessment [39, 153–156]. A vast body of research attests to the capability of these state-of-the-art sensors in identifying a multitude of biomolecular targets with precision, specificity, and in a label-free manner [157–161]. Over recent decades, innovations in FET biosensor design, especially for clinical diagnostics, have been monumental. Their remarkable electronic characteristics, combined with their compact nature and adaptability, make them ideal candidates for expedited label-free molecular detection. Furthermore, when infused with nanotechnologies, specifically nanoscale materials such as MNWs, their detection potential is notably augmented. Their scalable, top-tier production also establishes them as a primary option for sensing and evaluation platforms. Moreover, MNWs possess the capability to amplify the detection sensitivity and specificity of FET sensors substantially. Notwithstanding these advancements, there remain lingering challenges regarding the effectiveness and clinical implementation of transistor-based point-of-care (POC) devices.

Central to the operation of these biosensors is the semi-conductive route, designated as the “channel”, flanked by source–drain (S–D) electrodes. The presence of charged molecules atop the FET biosensors can influence the conductance in the S–D channel, which is subject to modulation by an electrostatically-coupled third gate electrode, operating through a slender dielectric partition [162–165]. Typically, oxide, such as  $\text{SiO}_2$  (Fig. 7a), acts as the gate dielectric with an underlying p-type silicon base [38]. Negative gate potential intensifies holes accumulation, increasing channel conductance, while its positive counterpart depletes holes, diminishing conductance. Molecular adsorption on the semiconductor channel either adjusts the local potential or

directly shifts the properties of the channel, varying the conductance of FET. This adaptability, enhanced sensitivity and real-time functionality distinguish the FET as an exemplary sensing apparatus. In contrast, solution-gated FET biosensors enable analyte identification in a liquid environment (Fig. 7a). Herein, semiconducting MNW pathways reside within a designated flow or sensory chamber. To prevent current leakage caused by ionic motions, insulating materials are employed on the source and electrodes. The submerged gate electrode, commonly composed of Ag/AgCl or Pt, is constrained by dimensional limitations, necessitating the utilization of miniaturized reference electrodes. At the channel-to-solution juncture, the gate potential is experienced across the confined breadth of the electric double-layer capacitance. It is the ionic makeup of the solution that dictates the thickness of this double layer, also known as the Debye length, which is generally in the vicinity of 1 nm.

MNW biosensors have gained significant traction for biomarker detection recently. However, direct detection from bodily fluids remains largely underexamined due to the intricacies of such media, signifying a diminished practical utility of these advanced nanobiosensors. Chang et al. [166] have developed a nanowire-based biosensing system designed for the rapid, label-free and electrical identification of cancer biomarkers, utilizing blood samples collected directly from capillaries (Fig. 7b). By passivating the MNW surface, they effectively negated the interference from non-specific binding during real-time evaluations in whole blood. Such passivated devices showcased notably reduced noise from unintended protein and biomaterial attachment in serum and exhibited heightened sensitivity toward designated biomarkers compared to their non-coated counterparts. The analytical sensitivity of these coated sensors in blood mirrored their performance in equivalent ionic-strength buffer solutions, indicating a negligible degradation in capability amidst the multifaceted medium. They then reliably detected a spectrum of cancer-linked markers at clinically relevant levels straight from capillary-sourced blood samples using their optimized system.

When looking into the design parameters, it becomes apparent that the necessity for nanostructured and low-roughness transparent electrodes is paramount. In their exploration, Ben-Sasson et al. succinctly outline the vertical field-effect transistor (VFET) structure, further elucidating the primary physics governing its operation [159]. Figure 7c offers a visual representation of the vertical FET design [161]. The VFET is constructed in a layered format, consisting of several key components: a gate (G), a gate dielectric layer, a source electrode (S), a semiconductor layer and a final drain contact (D). This design advantageously allows for the straightforward fabrication of devices with ultra-short channel lengths. For effective interaction among these components, the source electrode is required to be permeable to the vertical gate’s low-

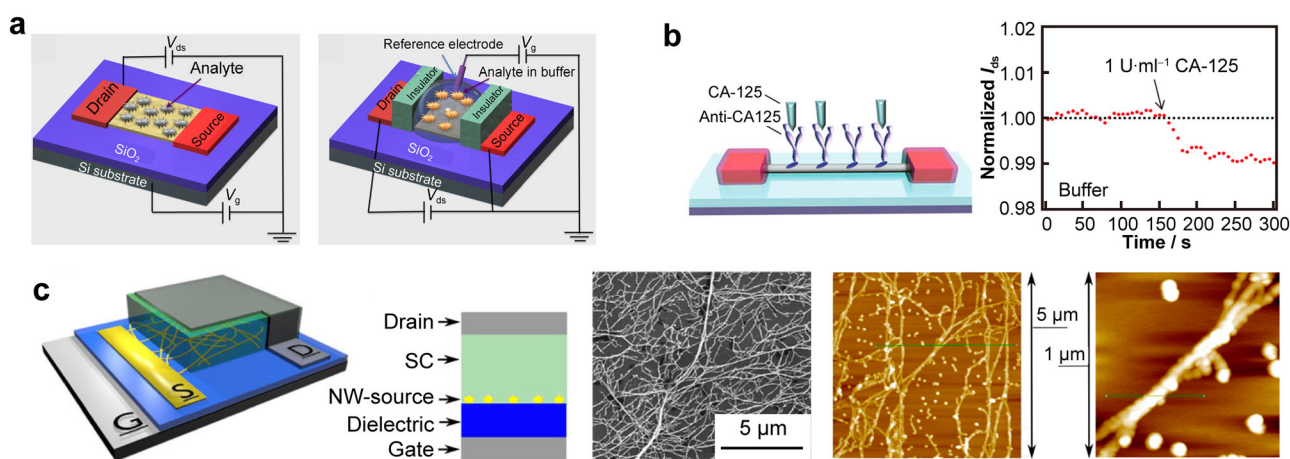


**Fig. 7** FET biosensors. **a** Conceptual diagram of FET biosensors (left: back-gated configuration, right: solution-gated configuration) employed for chemical-biological detection purposes. Reproduced with permission from Ref. [38]. Copyright 2018, Elsevier. **b** Different device architectures and corresponding real-time detection outcomes. Reproduced with permission from Ref. [162]. Copyright 2011, American Chemical Society. **c** (i) Illustration of Au/Ag metallic nanowire vertical organic field-effect transistor (MN-VOFET) configuration; (ii) detailed high-definition scanning electron microscopy (HDSEM) representation of intricate network of metallic nanowires; (iii) topography of nanowire film examined post a secondary stabilization submersion treatment through atomic force microscopy (AFM) imaging. Reproduced with permission from Ref. [161]. Copyright 2015, American Chemical Society

frequency or direct current (DC) electric fields. Further examination of the resultant film was conducted using atomic force microscopy (AFM), as explicated in Fig. 7c. It is notable that the maximum film thickness of the nanowires is below 30 nm, with a typical nanowire bundle measuring around 100 nm in width. The gaps between these bundles span several hundred nanometers. The obtained height-to-diameter ( $h/D$ ) ratio is kept sufficiently low to ensure an impressive on/off current ratio.

While transistor-based point-of-care devices, FET biosensors show promise, challenges persist in their effectiveness and clinical implementation. Achieving consistent reproducibility in device fabrication, minimizing variations and ensuring stability over time remain key challenges. Real-world applications require addressing environmental factors that can impact device performance. Standardization, affordability and user-friendliness are crucial for widespread clinical adoption. Moreover, issues related to sensitivity, specificity, and the validation of results in diverse clinical settings need careful consideration. A balanced perspective acknowledges these challenges and highlights the ongoing efforts to optimize transistor-based devices for reliable and accessible point-of-care diagnostics.

## 5 Outlooks

### 5.1 Machine learning

Machine learning possesses exceptional capacity for managing colossal datasets extracted from intricate

matrices in biosensing [167–171]. One prominent advantage is machine learning's ability to distill pertinent analytical conclusions from cluttered and low-resolution data, which might otherwise be obscured. Moreover, proficient execution of machine learning techniques elucidates intrinsic correlations between sample parameters and sensing signals and illuminates links between signals and biological events.

Specifically, machine learning can augment biosensor data analysis through several means. Figure 8a delineates machine learning's advantages [167, 172–174]. Algorithms may categorize sensing signals based on the target substance. On-field biosensor applications can introduce challenges due to matrix complexities and shifting operational conditions. External interferences, such as contamination, can significantly impact results. Machine learning can meticulously inspect the signal, affirm its veracity, and even compensate for deviations due to biofouling or other real-sample interferences. Since biosensor signals vary over seconds to minutes and electrical noise arises within seconds, machine learning models can distinguish genuine signals from this noise. These algorithms can reveal latent patterns, facilitating a more insightful comprehension of sensing data. Machine learning acts as a formidable instrument that boosts the swift, accurate and direct interpretation of biosensor data, crucial for on-site detection or diagnostic tasks. Figure 8b demonstrates machine learning's taxonomy [167].

Yu et al. [175] have suggested a methodology that integrates a sensor array with plasmonic nano sensors and employs machine learning algorithms to differentiate

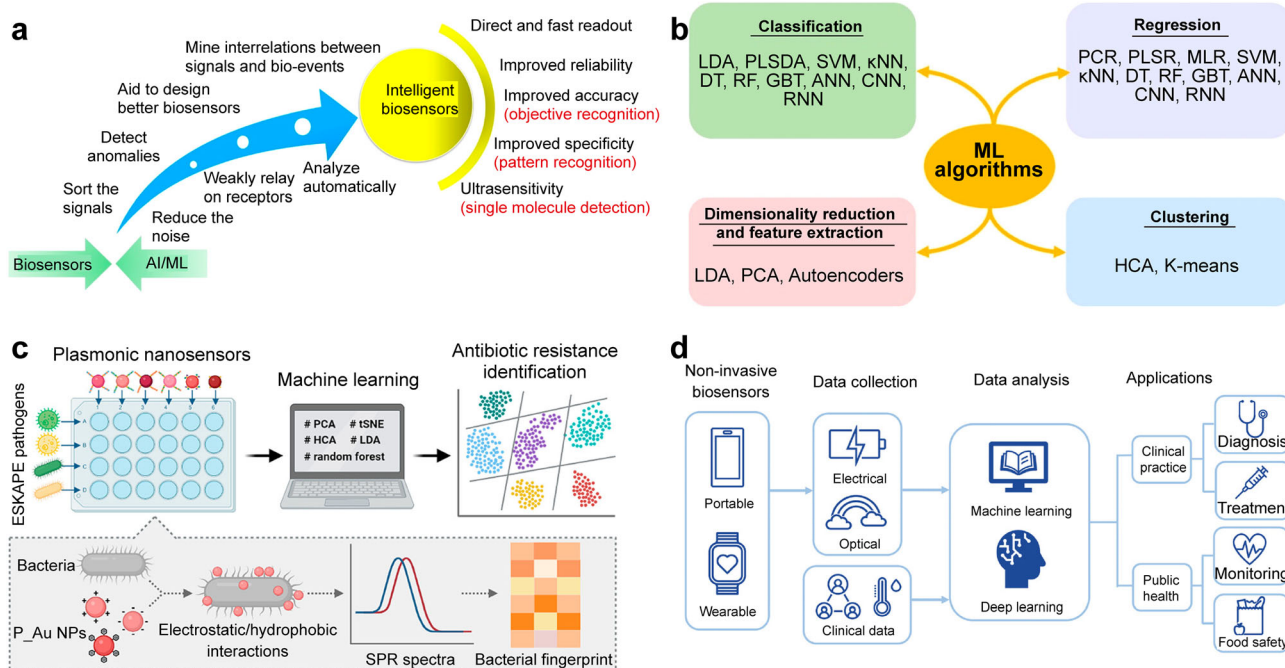


**Fig. 8** Applications and mechanisms of machine learning in enhancing biosensor functionality. **a** Benefits of biosensors amplified through machine learning; **b** decoding machine learning algorithms. Reproduced with permission from Ref. [167]. Copyright 2020, American Chemical Society. **c** Representation of ESKAPE pathogens resistance detection using plasmonic sensors integrated with machine learning. Reproduced with permission from Ref. [168]. Copyright 2023, American Chemical Society. **d** Overview of machine learning-enhanced biosensor operations. Reproduced with permission from Ref. [169]. Copyright 2021, John Wiley and Sons

between  $\beta$ -lactam antibiotic resistance among ESKAPE pathogens (Fig. 8c). The phenotypic differences between antibiotic-resistant and antibiotic-susceptible pathogens emanate from antibiotic hydrolases on their cell membranes/walls. To differentiate between these phenotypes, peptide-modified gold nanomaterials with varied surface charges and hydrophobic/hydrophilic characteristics are utilized. Bacterial binding affinities with peptides, contingent on their charge and hydrophilic/hydrophobic traits, dictate the surface plasmon resonance (SPR) spectrum, which serves as our signal metric. Employing machine learning facilitates the analysis of bacterial signatures from the plasmonic sensor array, distinguishing between antibiotic-resistant and susceptible strains in the ESKAPE pathogen. Both unsupervised and supervised machine learning methods identified antibiotic resistance in 12 ESKAPE pathogens with a remarkable accuracy rate of 89.74%. This research posits that gold MNWs might considerably amplify the sensitivity of plasmonic nano sensors, an aspect not extensively probed in current literature.

Figure 8d outlines and discusses the four fundamental components of machine learning-enhanced biosensors [176]. It underscores noninvasive biosensors' principles and dominant types, both portable and wearable, and delves into physiological signals from these biosensors, particularly focusing on electrical and optical signals. This

discussion then shifts to breakthroughs in machine learning-enhanced biosensors, spotlighting data handling methodologies. These techniques are examined across three tiers: preliminary data handling processing, traditional algorithms and state-of-the-art neural network-based algorithms.

The transformative potential of machine learning in nano sensor applications sets the stage for a profound shift toward the era of digital health. As machine learning algorithms enhance the capabilities of nano sensors, the synergy between data analytics and advanced sensing technologies propels us into a new frontier of healthcare innovation. This transition is not merely confined to the realm of diagnostics; rather, it marks the inception of a comprehensive digital health paradigm.

## 5.2 Era of digital health

The integration of nano sensors and machine learning not only refines our understanding of diseases at the molecular level but also lays the foundation for personalized healthcare strategies. In this era, the convergence of precise data analytics, real-time monitoring and predictive modeling promises a healthcare landscape characterized by proactive interventions, improved patient outcomes and a more interconnected and data-driven approach to well-being.

The advent of digital health, propelled by wearable technology and comprehensive data analytics, presents a novel opportunity to provide patients with instantaneous diagnostic capabilities and insights [177]. Mobile health (mHealth) devices that can detect a wide spectrum of biomarkers at minute concentrations in body fluids require the use of bio-affinity sensors. Such sensors predominantly employ “bioreceptors” for accurate target identification. The versatility of portable point-of-care testing (POCT) devices with affinity-based detection is evidenced in their wide range of applications, from continuous health tracking to precise disease diagnosis and management [174, 178]. Simultaneously, the rise of pliable and adaptable electronics in wearable systems over the recent decade heralds an innovative pathway for uninterrupted ambulatory data retrieval. This section charts the progressive trajectory of mHealth bio-affinity sensor technologies, tracing their evolution from preliminary laboratory assessments, transitioning to portable POCT tools and culminating in avant-garde wearable devices. Focus is directed toward the intricate detection mechanisms of mHealth affinity sensors, aided by bioreceptors such as antibodies, DNAs, aptamers and molecularly imprinted structures. Their associated signal transduction techniques, both electrochemical and optical, are also covered. This review concludes with a forward-looking perspective on the domain, pinpointing essential technological hurdles that must be navigated to spearhead a groundbreaking era in body-adherent affinity sensing platforms.

Historically, continuous sensing platforms utilizing tear fluids predominantly concentrated on glucose detection [176, 179]. Advancements in sensor technology have evolved from the early stages of flexible enzymatic sensing strips to the current integration of sensors within polymer-based contact lenses. Yao et al. [180] have been at the forefront, developing a contact lens sensor framework employing a Ti sol–gel process for enzyme immobilization, which resulted in heightened sensitivity. Further refinements led to the enhancement of these glucose-sensitive contact lenses, which now permit continuous monitoring of tear fluid through an embedded loop antenna and a wireless communication chipset embedded in the polymer matrix. Kim et al. [181, 182] have innovatively incorporated graphene with Ag MNWs to enhance the conductivity, optical transparency and flexibility of the contact lens sensors. By configuring graphene and nanowires as source-drain elements, along with a graphene channel FET on a biocompatible parylene substrate, they introduced a comprehensive soft-lens sensor system. This breakthrough enables remote, live glucose monitoring in rabbit eyes and in vitro intraocular pressure assessments using bovine eyes. However, the potential for these sensors to concurrently detect both glucose levels and pressure has yet to be investigated.

### 5.3 Flexible electronics

The emergence of wearable sensors marks a pivotal advancement toward individualized healthcare, providing the capability for uninterrupted physiological data acquisition, which is essential for timely preventive healthcare measures [183–187]. Nevertheless, the discrepancies in flexibility between traditional rigid electronics and the soft tissues in body frequently result in measurement inaccuracies during cutaneous monitoring. The advent of flexible electronics, characterized by their pliability and skin-like adaptability, facilitates seamless integration with human physiology. Advancements in the material science of MNWs are anticipated to propel research efforts within this domain significantly.

A quintessential flexible electronic device comprises several fundamental elements: the substrate, the active stratum, and the interfacing layer [174, 188]. The active layer, often derived from inorganic nanomaterials and fashioned via physical transference or solution-based methods, is acclaimed for its commendable physicochemical traits, charge carrier mobility and structural robustness. Flexible electronics, employing printed and transferred active components, have demonstrated considerable potential in physical detection tasks. For instance, a fusion of a nanowire transistor matrix and conductive, pressure-responsive rubber materializes into a system capable of tactile profiling [189]. These innovative sensors have been successfully attached as wearable patches for monitoring cutaneous temperature, cardiac electrical activity and various human motions.

## 6 Conclusion

This review reveals a promising trajectory in MNWs applications across diverse fields. As MNWs continue to emerge as versatile building blocks, the synthesis methods discussed, including template-based and template-free approaches, offer pathways for tailoring their properties. Ongoing advancements are expected to address challenges in scalability, uniformity, and environmentally friendly synthesis, fostering the integration of MNWs into various technologies. In the realm of sensors, MNWs’ unique characteristics, such as high aspect ratios and tunable properties, contribute to enhanced sensing performance. The exploration of novel procedures inspired by natural architectures showcases the potential for MNWs to mimic complex biological structures, opening avenues for innovative applications in fields like electronics, photonics, and catalysis.

As the field advances, ethical considerations, environmental implications, and sustainable synthesis methods

will be central to responsible MNW development. Collaboration across disciplines and transparent communication will be pivotal in navigating these challenges. Looking forward, the outlook is optimistic, envisioning MNWs as integral components in cutting-edge technologies, contributing to advancements in healthcare, energy, and beyond.

**Acknowledgements** This study was financially supported by the China Postdoctoral Science Foundation (No. 2023M742736).

#### Declarations

**Conflict of interest** The authors declare that they have no conflict of interest.

#### References

- [1] Wang N, Yang X, Zhang XX. Ultra robust subzero healable materials enabled by polyphenol nano-assemblies. *Nat Commun.* 2023;14(1):814. <https://doi.org/10.1038/s41467-023-36461-9>.
- [2] Fennell JF Jr, Liu SF, Azzarelli JM, Weis JG, Rochat S, Mirica KA, Ravensbaek JB, Swager TM. Nanowire chemical/biological sensors: status and a roadmap for the future. *Angew Chem Int Ed.* 2016;55(4):1266. <https://doi.org/10.1002/anie.201505308>.
- [3] Hong S, Lee H, Lee J, Kwon J, Han S, Suh YD, Cho H, Shin J, Yeo J, Ko SH. Highly stretchable and transparent metal nanowire heater for wearable electronics applications. *Adv Mater.* 2015;27(32):4744. <https://doi.org/10.1002/adma.201500917>.
- [4] Jiang Z, Nayeem MOG, Fukuda K, Ding S, Jin H, Yokota T, Inoue D, Hashizume D, Someya T. Highly stretchable metallic nanowire networks reinforced by the underlying randomly distributed elastic polymer nanofibers via interfacial adhesion improvement. *Adv Mater.* 2019;31(37):1903446. <https://doi.org/10.1002/adma.201903446>.
- [5] Zhou YL, Qu YP, Yin LT, Cheng WN, Huang YA, Fan RH. Coassembly of elastomeric microfibers and silver nanowires for fabricating ultra-stretchable microtextiles with weakly and tunable negative permittivity. *Compos Sci Technol.* 2022;223:109415. <https://doi.org/10.1016/j.compscitech.2022.109415>.
- [6] Zhou YL, Zhao CS, Wang JC, Li YZ, Li CX, Zhu HY, Feng SX, Cao ST, Kong DS. Stretchable high-permittivity nanocomposites for epidermal alternating-current electroluminescent displays. *ACS Mater Lett.* 2019;1(5):511. <https://doi.org/10.1021/acsmaterialslett.9b00376>.
- [7] Zhou YL, Cao ST, Wang J, Zhu HY, Wang JC, Yang SN, Wang X, Kong DS. Bright stretchable electroluminescent devices based on silver nanowire electrodes and high-k thermoplastic elastomers. *ACS Appl Mater Interfaces.* 2018;10(51):44760. <https://doi.org/10.1021/acsami.8b17423>.
- [8] Patil JJ, Chae WH, Trebach A, Carteer KJ, Lee E, Sannicolo T, Grossman JC. Failing forward: Stability of transparent electrodes based on metal nanowire networks. *Adv Mater.* 2021;33(5):2004356. <https://doi.org/10.1002/adma.202004356>.
- [9] Zhou GM, Xu L, Hu GW, Mai LQ, Cui Y. Nanowires for electrochemical energy storage. *Chem Rev.* 2019;119(20):11042. <https://doi.org/10.1021/acs.chemrev.9b00326>.
- [10] Cho IH, Kim DH, Park SS. Electrochemical biosensors: perspective on functional nanomaterials for on-site analysis. *Biomater Res.* 2020;24(1):1. <https://doi.org/10.1186/s40824-019-0181-y>.
- [11] Zhao HX, Zhou YL, Cao ST, Wang YF, Zhang JX, Feng SX, Wang JC, Li DC, Kong DS. Ultrastretchable and washable conductive microtextiles by coassembly of silver nanowires and elastomeric microfibers for epidermal human-machine interfaces. *ACS Mater Lett.* 2021;3(7):912. <https://doi.org/10.1021/acsmaterialslett.1c00128>.
- [12] Sannicolo T, Lagrange M, Cabos A, Celle C, Simonato JP, Bellet D. Metallic nanowire-based transparent electrodes for next generation flexible devices: a review. *Small.* 2016;12(44):6052. <https://doi.org/10.1002/sml.201602581>.
- [13] Zhou YL, Lian HX, Li ZL, Yin LT, Ji Q, Li K, Qi F. Crack engineering boosts the performance of flexible sensors. *View.* 2022;3(5):20220025. <https://doi.org/10.1002/VIW.20220025>.
- [14] Zhou YL, Cheng WN, Bai YZ, Hou C, Li K, Huang YA. Rise of flexible high-temperature electronics. *Rare Met.* 2023;42(6):1773. <https://doi.org/10.1007/s12598-023-02298-w>.
- [15] Wang YH, Yin L, Bai YZ, Liu SY, Wang L, Zhou Y, Hou C, Yang ZY, Wu H, Ma JJ, Shen YX, Deng PF, Zhang SH, Duan TJ, Ren JH, Xiao L, Yin ZP, Liu NS, Huang YA. Electrically compensated, tattoo-like electrodes for epidermal electrophysiology at scale. *Sci Adv.* 2020;6(43):eabd0996. <https://doi.org/10.1126/sciadv.abd0996>.
- [16] Qu YP, Zhou YL, Luo Y, Liu Y, Ding JF, Chen YL, Gong X, Yang JL, Peng Q, Qi XS. Universal paradigm of ternary metamaterials with tunable epsilon-negative and epsilon-near-zero response for perfect electromagnetic shielding. *Rare Met.* 2024;43(1):1. <https://doi.org/10.1007/s12598-023-02510-x>.
- [17] Bang J, Coskun S, Pyun KR, Doganay D, Tunca S, Koylan S, Kim D, Unal HE, Ko SH. Advances in protective layer-coating on metal nanowires with enhanced stability and their applications. *Appl Mater Today.* 2021;22:100909. <https://doi.org/10.1016/j.apmt.2020.100909>.
- [18] Yin JY, Wang SL, Di Carlo A, Chang A, Wan X, Xu J, Xiao X, Chen J. Smart textiles for self-powered biomonitoring. *Med-X.* 2023;1(3):3. <https://doi.org/10.1007/s44258-023-00001-3>.
- [19] Zhou YL, Yin LT, Xiang SF, Yu S, Johnson HM, Wang SL, Yin JY, Zhao J, Luo Y, Chu PK. Unleashing the potential of Mxene-based flexible materials for high-performance energy storage devices. *Adv Sci.* 2023;11(3):2304874. <https://doi.org/10.1002/advs.202304874>.
- [20] Zhai QF, Wang Y, Gong S, Ling YZ, Yap LW, Liu YY, Wang J, Simon GP, Cheng WL. Vertical gold nanowires stretchable electrochemical electrodes. *Anal Chem.* 2018;90(22):13498. <https://doi.org/10.1021/acs.analchem.8b03423>.
- [21] Lyu QX, Zhai QF, Dyson J, Gong S, Zhao YM, Ling YZ, Chandrasekaran R, Dong DS, Cheng WL. Real-time and in-situ monitoring of H<sub>2</sub>O<sub>2</sub> release from living cells by a stretchable electrochemical biosensor based on vertically aligned gold nanowire. *Anal Chem.* 2019;91(21):13521. <https://doi.org/10.1021/acs.analchem.9b02610>.
- [22] Zhai QF, Gong S, Wang Y, Lyu QX, Liu YY, Ling YZ, Wang J, Simon GP, Cheng WL. Enokitake mushroom-like standing gold nanowires toward wearable noninvasive bimodal glucose and strain sensing. *ACS Appl Mater Interfaces.* 2019;11(10):9724. <https://doi.org/10.1021/acsami.8b19383>.
- [23] Chen ZB, Jin HH, Yang ZG, He DP. Recent advances on bioreceptors and metal nanomaterials-based electrochemical impedance spectroscopy biosensors. *Rare Met.* 2023;42(4):1098. <https://doi.org/10.1007/s12598-022-02129-4>.
- [24] Huang YA, Wu H, Zhu C, Xiong WN, Chen FR, Xiao L, Liu JP, Wang KX, Li HA, Ye D. Programmable robotized 'transfer-and-jet' printing for large, 3D curved electronics on

- complex surfaces. *Int J Extreme Manuf.* 2021;3(4):045101. <https://doi.org/10.1088/2631-7990/ac115a>.
- [25] Abel B, Coskun S, Mohammed M, Williams R, Unalan HE, Aslan K. Metal-enhanced fluorescence from silver nanowires with high aspect ratio on glass slides for biosensing applications. *J Phys Chem C.* 2015;119(1):675. <https://doi.org/10.1021/jp509040f>.
- [26] Li Q, Lu N, Wang LH, Fan CH. Advances in nanowire transistor-based biosensors. *Small Methods.* 2018;2(4):1700263. <https://doi.org/10.1002/smt.201700263>.
- [27] Welch EC, Powell JM, Clevinger TB, Fairman AE, Shukla A. Advances in biosensors and diagnostic technologies using nanostructures and nanomaterials. *Adv Funct Mater.* 2021;31(44):2104126. <https://doi.org/10.1002/adfm.202104126>.
- [28] Guo SJ, Wang E. Noble metal nanomaterials: controllable synthesis and application in fuel cells and analytical sensors. *Nano Today.* 2011;6(3):240. <https://doi.org/10.1016/j.nantod.2011.04.007>.
- [29] Bai YZ, Yin LT, Hou C, Zhou YL, Zhang F, Xu ZY, Li K. Response regulation for epidermal fabric strain sensors via mechanical strategy. *Adv Funct Mater.* 2023;33(31):2214119. <https://doi.org/10.1002/adfm.202214119>.
- [30] Xu H, Shang HY, Wang C, Du YK. Ultrafine Pt-based nanowires for advanced catalysis. *Adv Funct Mater.* 2020;30(28):2000793. <https://doi.org/10.1002/adfm.202000793>.
- [31] Liao L, Wang SN, Xiao JJ, Bian XJ, Zhang YH, Scanlon M, Hu X, Tang Y, Liu B, Girault H. A nanoporous molybdenum carbide nanowire as an electrocatalyst for hydrogen evolution reaction. *Energy Environ Sci.* 2014;7(1):387. <https://doi.org/10.1039/C3EE42441C>.
- [32] Xiong WN, Feng H, Liwang HS, Yao WB, Duolikun D, Zhou YL, Huang YA. Multifunctional tactile feedbacks towards compliant robot manipulations via 3D-shaped electronic skin. *IEEE Sens J.* 2022;22(9):9046. <https://doi.org/10.1109/JSEN.2022.3162914>.
- [33] Li XL, Mo JS, Fang JR, Xu DX, Yang C, Zhang M, Li HB, Xie X, Hu N, Liu FM. Vertical nanowire array-based biosensors: device design strategies and biomedical applications. *J Mater Chem B.* 2020;8(34):7609. <https://doi.org/10.1039/D0TB00990C>.
- [34] Gupta R, Chauhan V, Gupta D, Goel S, Kumar R. Scaffold assisted synthesized metallic and semiconductor nanowires for electrochemical biosensing applications. *Multifaceted Bio--Sens Technol.* 2023;4:217. <https://doi.org/10.1016/B978-0-323-90807-8.00012-9>.
- [35] Chen Z, Wu CS, Yuan YX, Xie ZJ, Li TZ, Huang H, Li S, Deng JF, Lin HL, Shi Z, Li CZ, Hao YB, Tang YX, You YH, Al-Hartomy OA, Wageh S, Al-Sehemi AG, Lu RT, Zhang L, Lin XC, He YQ, Zhao GH, Li DF, Zhang H. CRISPR-Cas13a-powered electrochemical biosensor for the detection of the L452R mutation in clinical samples of SARS-CoV-2 variants. *J Nanobiotechnol.* 2023;21(1):141. <https://doi.org/10.1186/s12951-023-01903-5>.
- [36] Chen JJ, Chen Z, Meng CL, Zhou JX, Peng YH, Dai XQ, Li JF, Zhong YL, Chen XL, Yuan W, Ho HP, Gao BZ, Qu JL, Zhang XJ, Zhang H, Shao YH. CRISPR-powered optothermal nanotweezers: diverse bio-nanoparticle manipulation and single nucleotide identification. *Light Sci Appl.* 2023;12(1):273. <https://doi.org/10.1038/s41377-023-01326-9>.
- [37] Fennell JF Jr, Liu SF, Azzarelli JM, Weis JG, Rochat S, Mirica KA, Ravnsbæk JB, Swager TM. Nanowire chemical/biological sensors: status and a roadmap for the future. *Angew Chem Int Ed.* 2016;55(4):1266. <https://doi.org/10.1002/anie.201505308>.
- [38] Ahmad R, Mahmoudi T, Ahn MS, Hahn YB. Recent advances in nanowires-based field-effect transistors for biological sensor applications. *Biosens Bioelectron.* 2018;100:312. <https://doi.org/10.1016/j.bios.2017.09.024>.
- [39] Sadighbayan D, Hasanazadeh M, Ghafar-Zadeh E. Biosensing based on field-effect transistors (FET): recent progress and challenges. *TrAC Trends Anal Chem.* 2020;133:116067. <https://doi.org/10.1016/j.trac.2020.116067>.
- [40] Zhuo MP, Zhang YX, Li ZZ, Shi YL, Wang XD, Liao LS. Controlled synthesis of organic single-crystalline nanowires via the synergy approach of the bottom-up/top-down processes. *Nanoscale.* 2018;10(11):5140. <https://doi.org/10.1039/C7NR08931G>.
- [41] Isaacoff BP, Brown KA. Progress in top-down control of bottom-up assembly. *Nano Lett.* 2017;17(11):6508. <https://doi.org/10.1021/acs.nanolett.7b04479>.
- [42] Zhang Z, Wang JQ, Zhu YC. First principle study of electrical properties of Ce and S Co-doped SnO<sub>2</sub>. *Chin J Rare Met.* 2023;47(2):265. <https://doi.org/10.13373/j.cnki.cjrm.XY20060010>.
- [43] Raouf I, Khan A, Khalid S, Sohail M, Azad MM, Kim HS. Sensor-based prognostic health management of advanced driver assistance system for autonomous vehicles: a recent survey. *Mathematics.* 2022;10(18):3233. <https://doi.org/10.3390/math10183233>.
- [44] Hasan R, Hasan R. Pedestrian safety using the internet of things and sensors: issues, challenges, and open problems. *Futur Gener Comput Syst.* 2022;134:187. <https://doi.org/10.1016/j.future.2022.03.036>.
- [45] Serra A, Valles E. Advanced electrochemical synthesis of multicomponent metallic nanorods and nanowires: fundamentals and applications. *Appl Mater Today.* 2018;12:207. <https://doi.org/10.1016/j.apmt.2018.05.006>.
- [46] Graves JE, Bowker MEA, Summer A, Greenwood A, de León CP, Walsh FC. A new procedure for the template synthesis of metal nanowires. *Electrochem Commun.* 2018;87:58. <https://doi.org/10.1016/j.elecom.2017.11.022>.
- [47] Kaur A, Bajaj B, Kaushik A, Saini A, Sud D. A review on template assisted synthesis of multi-functional metal oxide nanostructures: status and prospects. *Mater Sci Eng B.* 2022;286:116005. <https://doi.org/10.1016/j.mseb.2022.116005>.
- [48] Pirotta KR, Navas D, Hernández-Velez M, Nielsch K, Vázquez M. Novel magnetic materials prepared by electrodeposition techniques: arrays of nanowires and multi-layered microwires. *J Alloy Compd.* 2004;369(1–2):18. <https://doi.org/10.1016/j.jallcom.2003.09.040>.
- [49] Sarkar J, Khan GG, Basumallick A. Nanowires: properties, applications and synthesis via porous anodic aluminium oxide template. *Bull Mater Sci.* 2007;30:271. <https://doi.org/10.1007/s12034-007-0047-0>.
- [50] Sulka GD, Brzózka A, Liu LF. Fabrication of diameter-modulated and ultrathin porous nanowires in anodic aluminum oxide templates. *Electrochim Acta.* 2011;56(14):4972. <https://doi.org/10.1016/j.electacta.2011.03.126>.
- [51] Kawamura G, Muto H, Matsuda A. Hard template synthesis of metal nanowires. *Front Chem.* 2014;2:104. <https://doi.org/10.3389/fchem.2014.00104>.
- [52] Wang ZG, Ding BQ. Engineering DNA self-assemblies as templates for functional nanostructures. *Acc Chem Res.* 2014;47(6):1654. <https://doi.org/10.1021/ar400305g>.
- [53] Kim YM, Kim JG, Noh Y, Kim WB. An overview of one-dimensional metal nanostructures for electrocatalysis. *Catal Surv Asia.* 2015;19:88. <https://doi.org/10.1007/s10563-015-9187-1>.
- [54] Bograchev DA, Volgin VM, Davydov AD. Simulation of inhomogeneous pores filling in template electrodeposition of ordered metal nanowire arrays. *Electrochim Acta.* 2013;112:279. <https://doi.org/10.1016/j.electacta.2013.08.171>.
- [55] Sofiah AGN, Samykano M, Kadrigama K, Mohan RV, Lah NAC. Metallic nanowires: mechanical properties-theory and



- experiment. *Appl Mater Today*. 2018;11:320. <https://doi.org/10.1016/j.apmt.2018.03.004>.
- [56] Wang KD, Wu C, Wang F, Liao MH, Jiang GQ. Bimetallic nanoparticles decorated hollow nanoporous carbon framework as nanozyme biosensor for highly sensitive electrochemical sensing of uric acid. *Biosens Bioelectron*. 2020;150:111869. <https://doi.org/10.1016/j.bios.2019.111869>.
- [57] Wang KD, Wu C, Wang F, Liu CM, Yu CJ, Jiang GQ. In-situ insertion of carbon nanotubes into metal-organic frameworks-derived  $\alpha$ -Fe<sub>2</sub>O<sub>3</sub> polyhedrons for highly sensitive electrochemical detection of nitrite. *Electrochim Acta*. 2018;285:128. <https://doi.org/10.1016/j.electacta.2018.07.228>.
- [58] Kouhpanji MRZ, Stadler BJH. Projection method as a probe for multiplexing/demultiplexing of magnetically enriched biological tissues. *RSC Adv*. 2020;10(22):13286. <https://doi.org/10.1039/D0RA01574A>.
- [59] Chen FR, Gai MX, Sun NN, Xu ZY, Liu L, Yu HY, Bian J, Huang YA. Laser-driven hierarchical “gas-needles” for programmable and high-precision proximity transfer printing of microchips. *Sci Adv*. 2023;9(43):eadk0244. <https://doi.org/10.1126/sciadv.adk0244>.
- [60] Zhuang CQ, Qi HY, Cheng X, Chen G, Gao CL, Wang LH, Sun SR, Zou J, Han XD. In Situ observation of dynamic galvanic replacement reactions in twinned metallic nanowires by liquid cell transmission electron microscopy. *Angew Chem Int Ed*. 2019;58(51):18627. <https://doi.org/10.1002/anie.201910379>.
- [61] Cui F, Yu Y, Dou LT, Sun JW, Yang Q, Schildknecht C, Schierle-Armdt K, Yang PD. Synthesis of ultrathin copper nanowires using tris (trimethylsilyl) silane for high-performance and low-haze transparent conductors. *Nano Lett*. 2015;15(11):7610. <https://doi.org/10.1021/acs.nanolett.5b03422>.
- [62] Kim KH, Jang NS, Ha SH, Cho JH, Kim JM. Highly sensitive and stretchable resistive strain sensors based on microstructured metal nanowire/elastomer composite films. *Small*. 2018;14(14):1704232. <https://doi.org/10.1002/sml.201704232>.
- [63] Yang ZW, Fu LQ, Wang SL, Zhang M, Wang Y, Ma ZQ, Wang DP. Balance of strength and plasticity of additive manufactured Ti-6Al-4V alloy by forming TiB whiskers with cyclic gradient distribution. *Addit Manuf*. 2021;39:101883. <https://doi.org/10.1016/j.addma.2021.101883>.
- [64] Wang SL, Shan ZW, Huang H. The mechanical properties of nanowires. *Adv Sci*. 2017;4(4):1600332. <https://doi.org/10.1002/advs.201600332>.
- [65] Kumar GU, Suresh S, Thansekhar MR, Halpati D. Role of inter-nanowire distance in metal nanowires on pool boiling heat transfer characteristics. *J Colloid Interface Sci*. 2018;532:218. <https://doi.org/10.1016/j.jcis.2018.07.092>.
- [66] Ma JJ, Wang K, Zhan MS. Growth mechanism and electrical and magnetic properties of Ag-Fe<sub>3</sub>O<sub>4</sub> core-shell nanowires. *ACS Appl Mater Interfaces*. 2015;7(29):16027. <https://doi.org/10.1021/acsami.5b04342>.
- [67] Jany BR, Janas A, Krok F. Retrieving the quantitative chemical information at nanoscale from scanning electron microscope energy dispersive X-ray measurements by machine learning. *Nano Lett*. 2017;17(11):6520. <https://doi.org/10.1021/acs.nanolett.7b01789>.
- [68] Hong WH, Wang J, Wang E. Facile synthesis of Pt Cu nanowires with enhanced electrocatalytic activity. *Nano Res*. 2015;8:2308. <https://doi.org/10.1007/s12274-015-0741-y>.
- [69] Wang K, Wu C, Wang F, Jing N, Jiang G. Co/Co<sub>3</sub>O<sub>4</sub> nanoparticles coupled with hollow nanoporous carbon polyhedrons for the enhanced electrochemical sensing of acetaminophen. *ACS Sustain Chem Eng*. 2019;7(22):18582. <https://doi.org/10.1021/acssuschemeng.9b04813>.
- [70] Wang KD, Wu C, Wang F, Jiang GQ. MOF-derived CoP X nanoparticles embedded in nitrogen-doped porous carbon polyhedrons for nanomolar sensing of p-nitrophenol. *ACS Appl Nano Mater*. 2018;1(10):5843. <https://doi.org/10.1021/acsnm.8b01501>.
- [71] Shi LJ, Wang RR, Zhai HT, Liu YQ, Gao L, Sun J. A long-term oxidation barrier for copper nanowires: graphene says yes. *Phys Chem Chem Phys*. 2015;17(6):4231. <https://doi.org/10.1039/C4CP05187D>.
- [72] Desimoni E, Brunetti B. X-ray photoelectron spectroscopic characterization of chemically modified electrodes used as chemical sensors and biosensors: a review. *Materials*. 2015;3(2):70. <https://doi.org/10.3390/chemosensors3020070>.
- [73] Bredar ARC, Chown AL, Burton AR, Farnum BH. Electrochemical impedance spectroscopy of metal oxide electrodes for energy applications. *ACS Appl Energy Mater*. 2020;3(1):66. <https://doi.org/10.1021/acsaem.9b01965>.
- [74] Chen J, Arianpour B, Wang KD, Wang SL, Yin JY, Zhang YR, Zhu E, Hsiai TK. Emerging nanomaterials to enhance electrochemical impedance spectroscopy for biomedical applications. *Front Mater*. 2023;10:1146045. <https://doi.org/10.3389/fmats.2023.1146045>.
- [75] Li CL, Iqbal M, Lin JJ, Luo XL, Jiang B, Malgras V, Wu KCW, Kim J, Yamauchi Y. Electrochemical deposition: an advanced approach for templated synthesis of nanoporous metal architectures. *Acc Chem Res*. 2018;51(8):1764. <https://doi.org/10.1021/acs.accounts.8b00119>.
- [76] Gambirasi A, Cattarin S, Musiani M, Vázquez-Gómez L, Verlato E. Direct electrodeposition of metal nanowires on electrode surface. *Electrochim Acta*. 2011;56(24):8582. <https://doi.org/10.1016/j.electacta.2011.07.045>.
- [77] Md Jani AM, Habiballah AS, Budiman Abdul Halim MZ, Ahmad Zulkifli FW, Mahmud AH, Yazid H. Nanoporous anodic aluminum oxide (NAAO) for Catalytic, biosensing and template synthesis applications (a review). *Curr Nanosci*. 2019;15(1):49. <https://doi.org/10.2174/1573413714666180308145336>.
- [78] Salvatore KL, Wong SS. Exploring strategies toward synthetic precision control within core-shell nanowires. *Acc Chem Res*. 2021;54(11):2565. <https://doi.org/10.1021/acs.accounts.1c00041>.
- [79] Merkel TJ, Herlihy KP, Nunes J, Orgel RM, Rolland JP, Desimone JM. Scalable, shape-specific, top-down fabrication methods for the synthesis of engineered colloidal particles. *Langmuir*. 2010;26(16):13086. <https://doi.org/10.1021/la903890h>.
- [80] Jones MR, Osberg KD, Macfarlane RJ, Langille MR, Mirkin CA. Templated techniques for the synthesis and assembly of plasmonic nanostructures. *Chem Rev*. 2011;111(6):3736. <https://doi.org/10.1021/cr1004452>.
- [81] Xue Y, Chen S, Yu JR, Bunes BR, Xue ZX, Xu JK, Lu BY, Zang L. Nanostructured conducting polymers and their composites: synthesis methodologies, morphologies and applications. *J Mater Chem C*. 2020;8(30):10136. <https://doi.org/10.1039/D0TC02152K>.
- [82] Scott JA, Totonjian D, Martin AA, Tran TT, Fang JH, Toth M, McDonagh AM, Aharonovich I, Lobo CJ. Versatile method for template-free synthesis of single crystalline metal and metal alloy nanowires. *Nanoscale*. 2016;8(5):2804. <https://doi.org/10.1039/C5NR07307C>.
- [83] Pruneanu S, Olenic L, Farha Al-Said SA, Borodi G, Houlton A, Horrocks BR. Template and template-free preparation of one-dimensional metallic nanostructures. *J Mater Sci*. 2010;45:3151. <https://doi.org/10.1007/s10853-010-4320-z>.
- [84] Sarkar R, Farghaly AA, Arachchige IU. Oxidative self-assembly of Au/Ag/Pt Alloy nanoparticles into high-surface area, mesoporous, and conductive aerogels for methanol electro-oxidation. *Chem Mater*. 2022;34(13):5874. <https://doi.org/10.1021/acs.chemmater.2c00717>.

- [85] Young C, Wang J, Kim J, Sugahara Y, Henzie J, Yamauchi Y. Controlled chemical vapor deposition for synthesis of nanowire arrays of metal-organic frameworks and their thermal conversion to carbon/metal oxide hybrid materials. *Chem Mater.* 2018;30(10):3379. <https://doi.org/10.1021/acs.chemmater.8b00836>.
- [86] Wang XR, Yushin G. Chemical vapor deposition and atomic layer deposition for advanced lithium ion batteries and supercapacitors. *Energy Environ Sci.* 2015;8(7):1889. <https://doi.org/10.1039/C5EE01254F>.
- [87] Tang ML, Wang GD, Wu SH, Xiang Y. One-step preparation of Si-doped ultra-long b-Ga<sub>2</sub>O<sub>3</sub> nanowires by low-pressure chemical vapor deposition. *Crystals.* 2023;13(6):898. <https://doi.org/10.3390/cryst13060898>.
- [88] Barth S, Hernandez-Ramirez F, Holmes JD, Romano-Rodríguez A. Synthesis and applications of one-dimensional semiconductors. *Prog Mater Sci.* 2010;55(6):563. <https://doi.org/10.1016/j.pmatsci.2010.02.001>.
- [89] Won D, Bang J, Choi SH, Pyun KR, Jeong S, Lee Y, Ko SH. Transparent electronics for wearable electronics application. *Chem Rev.* 2023;123(16):9982. <https://doi.org/10.1021/acs.chemrev.3c00139>.
- [90] LaMer VK, Dinegar RH. Theory, production and mechanism of formation of monodispersed hydrosols. *J Am Chem Soc.* 1950;72(11):4847. <https://doi.org/10.1021/ja01167a001>.
- [91] Lin JY, Hsueh YL, Huang JJ, Wu JR. Effect of silver nitrate concentration of silver nanowires synthesized using a polyol method and their application as transparent conductive films. *Thin Solid Films.* 2015;584:243. <https://doi.org/10.1016/j.tsf.2015.02.067>.
- [92] Moon H, Won P, Lee J, Ko SH. Low-haze, annealing-free, very long Ag nanowire synthesis and its application in a flexible transparent touch panel. *Nanotechnology.* 2016;27(29):295201. <https://doi.org/10.1088/0957-4484/27/29/295201>.
- [93] Sim H, Kim C, Bok S, Kim MK, Oh H, Lim GH, Cho SM, Lim B. Five-minute synthesis of silver nanowires and their roll-to-roll processing for large-area organic light emitting diodes. *Nanoscale.* 2018;10(25):12087. <https://doi.org/10.1039/C8NR02242A>.
- [94] Zhang T, Zheng M, Li HJ, Yuan TC, Peng HZ, Wang KD, Zhan XX, Liu YQ, Wang KL, Liu XR, Li YJ. Photochromic transparent bamboo composite with excellent optical and thermal management for smart window applications. *Ind Crops Prod.* 2023;205:117532. <https://doi.org/10.1016/j.indcrop.2023.117532>.
- [95] Liu XR, Peng HZ, Zhang T, Wang KL, Dong YM, Wang KD, Zhan XX, Liu YQ, Li YJ, Li JZ. One-step brush-coating strategy for low-haze and water-resistant transparent wood films. *Prog Org Coat.* 2023;185:107912. <https://doi.org/10.1016/j.porgcoat.2023.107912>.
- [96] Hsu PC, Wang S, Wu H, Narasimhan VK, Kong DS, Ryoung Lee H, Cui Y. Performance enhancement of metal nanowire transparent conducting electrodes by mesoscale metal wires. *Nat Commun.* 2013;4(1):2522. <https://doi.org/10.1038/ncomms3522>.
- [97] Lee MS, Lee K, Kim SY, Lee H, Park J, Choi KH, Kim HK, Kim DG, Lee DY, Nam SW, Park JU. High-performance, transparent, and stretchable electrodes using graphene-metal nanowire hybrid structures. *Nano Lett.* 2013;13(6):2814. <https://doi.org/10.1021/nl401070p>.
- [98] Choi C, Cai J, Lee C, Lee HM, Xu MJ, Huang Y. Intimate atomic Cu-Ag interfaces for high CO<sub>2</sub> RR selectivity towards CH<sub>4</sub> at low over potential. *Nano Res.* 2021;14:3497. <https://doi.org/10.1007/s12274-021-3639-x>.
- [99] Zhu E, Liu Y, Huang J, Zhang A, Peng B, Liu Z, Liu H, Yu J, Li YR, Yang L. Bubble-mediated large-scale hierarchical assembly of ultrathin Pt nanowire network monolayer at gas/liquid interfaces. *ACS Nano.* 2023;17(14):14152. <https://doi.org/10.1021/acsnano.3c04771>.
- [100] Wang SL, Cui QY, Abiri P, Roustaei M, Zhu E, Li YR, Wang KD, Duarte S, Yang LL, Ebrahimi R, Bersohn M, Chen J, Hsiai TK. A self-assembled implantable microtubular pacemaker for wireless cardiac electrotherapy. *Sci Adv.* 2023;9(42):540. <https://doi.org/10.1126/sciadv.adj0540>.
- [101] Wang L, Gong CC, Yuan XZ, Wei G. Controlling the self-assembly of biomolecules into functional nanomaterials through internal interactions and external stimulations: a review. *Nanomaterials.* 2019;9(2):285. <https://doi.org/10.3390/nano9020285>.
- [102] Gong C, Sun SW, Zhang YJ, Sun L, Su ZQ, Wu AG, Wei G. Hierarchical nanomaterials via biomolecular self-assembly and bioinspiration for energy and environmental applications. *Nanoscale.* 2019;11(10):4147. <https://doi.org/10.1039/C9NR00218A>.
- [103] Bai Y, Luo Q, Liu JQ. Protein self-assembly via supramolecular strategies. *Chem Soc Rev.* 2016;45(10):2756. <https://doi.org/10.1039/C6CS00004E>.
- [104] Zha AY, Zha QB, Li Z, Zhang HM, Ma XF, Xie W, Zhu MS. Surfactant-enhanced electrochemical detection of bisphenol A based on Au on ZnO/reduced graphene oxide sensor. *Rare Met.* 2023;42(4):1274. <https://doi.org/10.1007/s12598-022-02172-1>.
- [105] Lu W, Lieber CM. Nanoelectronics from the bottom up. *Nat Mater.* 2007;6(11):841. <https://doi.org/10.1038/nmat2028>.
- [106] Li Y, Fang T, Zhang J, Zhu H, Sun Y, Wang S, Lu Y, Kong D. Ultrasensitive and ultrastretchable electrically self-healing conductors. *Proc Natl Acad Sci.* 2023;120(23):e2300953120. <https://doi.org/10.1073/pnas.2300953120>.
- [107] Hu G, Zhu H, Guo H, Wang S, Sun Y, Zhang J, Lin Y, Kong D. Maskless fabrication of highly conductive and ultrastretchable liquid metal features through selective laser activation. *ACS Appl Mater Interfaces.* 2023;15(23):28675. <https://doi.org/10.1021/acsami.3c06308>.
- [108] Jung WB, Jang S, Cho SY, Jeon HJ, Jung HT. Recent progress in simple and cost-effective top-down lithography for  $\approx 10$  nm scale nanopatterns: from edge lithography to secondary sputtering lithography. *Adv Mater.* 2020;32(35):1907101. <https://doi.org/10.1002/adma.201907101>.
- [109] Poolakkandy RR, Menampambath MM. Soft-template-assisted synthesis: a promising approach for the fabrication of transition metal oxides. *Nanoscale Adv.* 2020;2(11):5015. <https://doi.org/10.1039/D0NA00599A>.
- [110] Yaman M, Khudiyev T, Ozgur E, Kanik M, Aktas O, Ozgur EO, Deniz H, Korkut E, Bayindir M. Arrays of indefinitely long uniform nanowires and nanotubes. *Nat Mater.* 2011;10(7):494. <https://doi.org/10.1038/nmat3038>.
- [111] Gregorczyk K, Knez M. Hybrid nanomaterials through molecular and atomic layer deposition: top down, bottom up, and in-between approaches to new materials. *Prog Mater Sci.* 2016;75:1. <https://doi.org/10.1016/j.pmatsci.2015.06.004>.
- [112] Persano L, Camposo A, Pisignano D. Integrated bottom-up and top-down soft lithographies and microfabrication approaches to multifunctional polymers. *J Mater Chem C.* 2013;1(46):7663. <https://doi.org/10.1039/C3TC30978A>.
- [113] Morag A, Jelinek R. "Bottom-up" transparent electrodes. *J Colloid Interface Sci.* 2016;482:267. <https://doi.org/10.1016/j.jcis.2016.07.079>.
- [114] Nerowski A, Opitz J, Baraban L, Cuniberti G. Bottom-up synthesis of ultrathin straight platinum nanowires: electric field impact. *Nano Res.* 2013;6:303. <https://doi.org/10.1007/s12274-013-0303-0>.
- [115] Zhao ZH, Shi B, Wang T, Wang RM, Chang Q, Yun JJ, Zhang LM, Wu HJ. Microscopic and macroscopic structural strategies for enhancing microwave absorption in MXene-based



- composites. *Carbon*. 2023;215:118450. <https://doi.org/10.1016/j.carbon.2023.118450>.
- [116] Yan W, Page A, Nguyen-Dang T, Qu YP, Sordo F, Wei L, Sorin F. Advanced multimaterial electronic and optoelectronic fibers and textiles. *Adv Mater*. 2019;31(1):1802348. <https://doi.org/10.1002/adma.201802348>.
- [117] Han J, Yang J, Gao W, Bai H. Ice-templated, large-area silver nanowire pattern for flexible transparent electrode. *Adv Funct Mater*. 2021;31(16):2010155. <https://doi.org/10.1002/adfm.202010155>.
- [118] Yang LX, Huang XJ, Wu HT, Liang YL, Ye M, Liu WC, Li FL, Xu T, Wang HC. Silver nanowires: from synthesis, growth mechanism, device fabrications to prospective engineered applications. *Eng Sci*. 2023;23:808. <https://doi.org/10.30919/es8d808>.
- [119] He Z, Wang JL, Chen SM, Liu JW, Yu SH. Self-assembly of nanowires: from dynamic monitoring to precision control. *Acc Chem Res*. 2022;55(11):1480. <https://doi.org/10.1021/acs.accounts.2c00052>.
- [120] Wang JL, Hassan M, Liu JW, Yu SH. Nanowire assemblies for flexible electronic devices: recent advances and perspectives. *Adv Mater*. 2018;30(48):1803430. <https://doi.org/10.1002/adma.201803430>.
- [121] Ye SR, Stewart IE, Chen ZF, Li B, Rathmell AR, Wiley BJ. How copper nanowires grow and how to control their properties. *Acc Chem Res*. 2016;49(3):442. <https://doi.org/10.1021/acs.accounts.5b00506>.
- [122] Tonelli D, Scavetta E, Gualandi I. Electrochemical deposition of nanomaterials for electrochemical sensing. *Sensors*. 2019;19(5):1186. <https://doi.org/10.3390/s19051186>.
- [123] García M, Batalla P, Escarpa A. Metallic and polymeric nanowires for electrochemical sensing and biosensing. *TrAC Trends Anal Chem*. 2014;57:6. <https://doi.org/10.1016/j.trac.2014.01.004>.
- [124] Li J, Xia B, Xiao X, Huang Z, Yin J, Jiang Y, Wang S, Gao H, Shi Q, Xie Y, Chen J. Stretchable thermoelectric fibers with three-dimensional interconnected porous network for low-grade body heat energy harvesting. *ACS Nano*. 2023;17(19):19232. <https://doi.org/10.1021/acsnano.3c05797>.
- [125] Kim MJ, Cruz MA, Yang F, Wiley BJ. Accelerating electrochemistry with metal nanowires. *Curr Opin Electrochem*. 2019;16:19. <https://doi.org/10.1016/j.coelec.2019.03.005>.
- [126] Fan Z, Zhang H. Crystal phase-controlled synthesis, properties and applications of noble metal nanomaterials. *Chem Soc Rev*. 2016;45(1):6. <https://doi.org/10.1039/C5CS00467E>.
- [127] Ye S, Rathmell AR, Chen Z, Stewart IE, Wiley BJ. Metal nanowire networks: the next generation of transparent conductors. *Adv Mater*. 2014;26(39):6670. <https://doi.org/10.1002/adma.201402710>.
- [128] Zhang SL, Bick M, Xiao X, Chen GR, Nashalian A, Chen J. Leveraging triboelectric nanogenerators for bioengineering. *Matter*. 2021;4(3):845. <https://doi.org/10.1016/j.matt.2021.01.006>.
- [129] Ye WX, Guo XL, Ma TL. A review on electrochemical synthesized copper-based catalysts for electrochemical reduction of CO<sub>2</sub> to C<sup>2+</sup> products. *Chem Eng J*. 2021;414:128825. <https://doi.org/10.1016/j.cej.2021.128825>.
- [130] Wu ZP, Lu XF, Zang SQ, Lou XW. Non-noble-metal-based electrocatalysts toward the oxygen evolution reaction. *Adv Funct Mater*. 2020;30(15):1910274. <https://doi.org/10.1002/adfm.201910274>.
- [131] Ahmad T, Liu S, Sajid M, Li K, Ali M, Liu L. Electrochemical CO<sub>2</sub> reduction to C<sup>2+</sup> products using Cu-based electrocatalysts: a review. *Nano Res Energy*. 2022;1(2):e9120021. <https://doi.org/10.26599/NRE.2022.9120021>.
- [132] Li J, Liang X, Cai L, Zhao CY. Surfactant-free synthesis of three-dimensional metallic nanonetworks via nanobubble-assisted self-assembly. *Langmuir*. 2021;37(27):8323. <https://doi.org/10.1021/acs.langmuir.1c01153>.
- [133] Patil JJ, Chae WH, Trebach A, Carter KJ, Lee E, Sannicola T, Grossman JC. Failing forward: stability of transparent electrodes based on metal nanowire networks. *Adv Mater*. 2021;33(5):2004356. <https://doi.org/10.1002/adma.202004356>.
- [134] Arefpour M, Kashi MA, Barzoki FK, Noormohammadi M, Ramazani A. Electrodeposited metal nanowires as transparent conductive electrodes: their release conditions, electrical conductivity, optical transparency and chemical stability. *Mater Des*. 2018;157:326. <https://doi.org/10.1016/j.matdes.2018.07.048>.
- [135] Stradiotto NR, Yamanaka H, Zanoni MVB. Electrochemical sensors: a powerful tool in analytical chemistry. *J Braz Chem Soc*. 2003;14(2):159. <https://doi.org/10.1590/S0103-50532003000200003>.
- [136] Dardano P, Rea I, De Stefano L. Microneedles-based electrochemical sensors: new tools for advanced biosensing. *Curr Opin Electrochem*. 2019;17:121. <https://doi.org/10.1016/j.coelec.2019.05.012>.
- [137] Li Y, Chen K, Pang Y, Zhang J, Wu M, Xu Y, Cao S, Zhang X, Wang S, Sun Y. Multifunctional microneedle patches via direct ink drawing of nanocomposite inks for personalized transdermal drug delivery. *ACS Nano*. 2023;17(20):19925. <https://doi.org/10.1021/acsnano.3c04758>.
- [138] Zhu C, Xu ZY, Hou C, Lv XD, Jiang S, Ye D, Huang YA. Flexible, monolithic piezoelectric sensors for large-area structural impact monitoring via MUSIC-assisted machine learning. *Struct Health Monit*. 2023;23(1):121. <https://doi.org/10.1177/14759217231161812>.
- [139] Yin ZP, Huang YA, Yang H, Chen JK, Duan YQ, Chen W. Flexible electronics manufacturing technology and equipment. *Sci China Technol Sci*. 2022;65(9):1940. <https://doi.org/10.1007/s11431-022-2098-1>.
- [140] Gokhale AA, Lu J, Weerasiri RR, Yu J, Lee I. Amperometric detection and quantification of nitrate ions using a highly sensitive nanostructured membrane electrocodeposited biosensor array. *Electroanalysis*. 2015;27(5):1127. <https://doi.org/10.1002/elan.201400547>.
- [141] Lu Y, Wang MY, Wang DY, Sun YH, Liu ZH, Gao RK, Yu LD, Zhang DZ. Flexible impedance sensor based on Ti<sub>3</sub>C<sub>2</sub>T<sub>x</sub> MXene and graphitic carbon nitride nanohybrid for humidity-sensing application with ultrahigh response. *Rare Met*. 2023;42(7):2204. <https://doi.org/10.1007/s12598-023-02268-2>.
- [142] Chen YZ, Chen Z, Li TZ, Qiu M, Zhang JH, Wang Y, Yuan W, Ho-Pui Ho A, Al-Hartomy O, Wageh S, Al-Sehemi AG, Shi X, Li JF, Xie ZJ, Li XJ, Zhang H. Ultrasensitive and specific clustered regularly interspaced short palindromic repeats empowered a plasmonic fiber tip system for amplification-free monkeypox virus detection and genotyping. *ACS Nano*. 2023;17(13):12903. <https://doi.org/10.1021/acsnano.3c05007>.
- [143] Shen JN, Chen Z, Xie RB, Li JF, Liu CY, He YQ, Ma XP, Yang H, Xie ZJ. CRISPR/Cas12a-assisted isothermal amplification for rapid and specific diagnosis of respiratory virus on a microfluidic platform. *Biosens Bioelectron*. 2023;237:115523. <https://doi.org/10.1016/j.bios.2023.115523>.
- [144] Wu Y, Gao M, Li S, Ren Y, Qin G. Copper wires with seamless 1D nanostructures: preparation and electrochemical sensing performance. *Mater Lett*. 2018;211:247. <https://doi.org/10.1016/j.matlet.2017.10.016>.
- [145] Patella B, Russo R, O'Riordan A, Aiello G, Sunseri C, Inguanta R. Copper nanowire array as highly selective electrochemical sensor of nitrate ions in water. *Talanta*. 2021;221:121643. <https://doi.org/10.1016/j.talanta.2020.121643>.
- [146] Ju L, Wu G, Lu B, Li X, Wu H, Liu A. Non-enzymatic amperometric glucose sensor based on copper nanowires

- decorated reduced graphene oxide. *Electroanalysis*. 2016; 28(10):2543. <https://doi.org/10.1002/elan.201600100>.
- [147] Ramulu T, Venu R, Sinha B, Lim B, Jeon S, Yoon S, Kim C. Nanowires array modified electrode for enhanced electrochemical detection of nucleic acid. *Biosens Bioelectron*. 2013; 40(1):258. <https://doi.org/10.1016/j.bios.2012.07.034>.
- [148] Li X, Qin Z, Fu H, Li T, Peng R, Li Z, Rini JM, Liu X. Enhancing the performance of paper-based electrochemical impedance spectroscopy nanobiosensors: an experimental approach. *Biosens Bioelectron*. 2021;177:112672. <https://doi.org/10.1016/j.bios.2020.112672>.
- [149] Yin J, Geng Q, Xiao X, Wang S, Meng L, Deng N, Xu J, Su B, Chen J, Zhao W. Mussel-inspired antibacterial sponge for highly efficient water purification and sterilization. *J Hazard Mater*. 2024;461:132598. <https://doi.org/10.1016/j.jhazmat.2023.132598>.
- [150] Satta S, Rockwood SJ, Wang K, Wang S, Mozneb M, Arzt M, Hsiai TK, Sharma A. Microfluidic organ-chips and stem cell models in the fight against COVID-19. *Circ Res*. 2023;132(10):1405. <https://doi.org/10.1161/CIRCRESAHA.122.321877>.
- [151] Kalkman GA, Zhang Y, Monachino E, Mathwig K, Kamminga ME, Pourhossein P, Oomen PE, Stratmann SA, Zhao Z, van Oijen AM. Bisecting microfluidic channels with metallic nanowires fabricated by nanoskiving. *ACS Nano*. 2016;10(2):2852. <https://doi.org/10.1021/acsnano.5b07996>.
- [152] Li X, Zhao C, Liu X. A paper-based microfluidic biosensor integrating zinc oxide nanowires for electrochemical glucose detection. *Microsyst Nanoeng*. 2015;1(1):1. <https://doi.org/10.1038/micronano.2015.14>.
- [153] Syedmoradi L, Ahmadi A, Norton ML, Omidfar K. A review on nanomaterial-based field effect transistor technology for biomarker detection. *Microchim Acta*. 2019;186:1. <https://doi.org/10.1007/s00604-019-3850-6>.
- [154] Sinha A, Tai TY, Li KH, Gopinathan P, Chung YD, Sarangadharan I, Ma HP, Huang PC, Shiesh SC, Wang YL. An integrated microfluidic system with field-effect-transistor sensor arrays for detecting multiple cardiovascular biomarkers from clinical samples. *Biosens Bioelectron*. 2019;129:155. <https://doi.org/10.1016/j.bios.2019.01.001>.
- [155] Yu H, Gai M, Liu L, Chen F, Huang Y. Laser-induced direct graphene patterning: from formation mechanism to flexible applications. *Soft Sci*. 2023;3(1):4. <https://doi.org/10.1016/j.mattod.2023.10.009>.
- [156] Xiong WN, Zhu C, Guo DL, Hou C, Yang ZX, Xu ZY, Qiu L, Yang H, Li K, Huang YA. Bio-inspired, intelligent flexible sensing skin for multifunctional flying perception. *Nano Energy*. 2021;90:106550. <https://doi.org/10.1016/j.nanoen.2021.106550>.
- [157] Wang K, Huang K, Jiang G. Enhanced removal of aqueous acetaminophen by a laccase-catalyzed oxidative coupling reaction under a dual-pH optimization strategy. *Sci Total Environ*. 2018;616:1270. <https://doi.org/10.1016/j.scitotenv.2017.10.191>.
- [158] Li H, Shi W, Song J, Jang HJ, Dailey J, Yu J, Katz HE. Chemical and biomolecule sensing with organic field-effect transistors. *Chem Rev*. 2018;119(1):3. <https://doi.org/10.1021/acs.chemrev.8b00016>.
- [159] Ben-Sasson AJ, Azulai D, Gilon H, Facchetti A, Markovich G, Tessler N. Self-assembled metallic nanowire-based vertical organic field-effect transistor. *ACS Appl Mater Interfaces*. 2015;7(4):2149. <https://doi.org/10.1021/am505174p>.
- [160] Wang YH, Tang TY, Xu YZ, Yin L, Li G, Zhang HM, Liu HC, Huang YA. All-weather, natural silent speech recognition via machine-learning-assisted tattoo-like electronics. *NPJ Flex Electron*. 2021;5(1):20. <https://doi.org/10.1038/s41528-021-00119-7>.
- [161] Gai LY, Lai RP, Dong XH, Wu X, Luan QT, Wang J, Lin HF, Ding WH, Wu GL, Xie WF. Recent advances in ethanol gas sensors based on metal oxide semiconductor heterojunctions. *Rare Met*. 2022;41(6):1818. <https://doi.org/10.1007/s12598-021-01937-4>.
- [162] Shoorideh K, Chui CO. On the origin of enhanced sensitivity in nanoscale FET-based biosensors. *Proc Natl Acad Sci*. 2014; 111(14):5111. <https://doi.org/10.1073/pnas.131548511>.
- [163] Wang Q, Zhang G, Zhang HY, Duan YQ, Yin ZP, Huang YA. High-resolution, flexible, and full-color perovskite image photodetector via electrohydrodynamic printing of ionic-liquid-based ink. *Adv Funct Mater*. 2021;31(28):2100857. <https://doi.org/10.1002/adfm.202100857>.
- [164] Wang YH, Yin L, Bai YZ, Liu S, Wang L, Zhou Y, Hou C, Yang ZY, Wu H, Ma JJ, Shen YX, Deng PF, Zhang S, Duan TJ, Li Z, Ren JH, Xiao L, Yin ZP, Lu NS, Huang YA. Electrically compensated, tattoo-like electrodes for epidermal electrophysiology at scale. *Sci Adv*. 2020;6(43):eabd0996. <https://doi.org/10.1126/sciadv.abd0996>.
- [165] Huang YA, Zhu C, Xiong WN, Wang Y, Jiang YG, Qiu L, Guo DL, Hou C, Jiang S, Yang ZX, Wang B, Wang L, Yin ZP. Flexible smart sensing skin for “Fly-by-Feel” morphing aircraft. *Sci China Technol Sci*. 2022;65(1):1. <https://doi.org/10.1007/s11431-020-1793-0>.
- [166] Chang HK, Ishikawa FN, Zhang R, Datar R, Cote RJ, Thompson ME, Zhou C. Rapid, label-free, electrical whole blood bioassay based on nanobiosensor systems. *ACS Nano*. 2011;5(12):9883. <https://doi.org/10.1021/nn2035796>.
- [167] Cui F, Yue Y, Zhang Y, Zhang Z, Zhou HS. Advancing biosensors with machine learning. *ACS Sens*. 2020;5(11):3346. <https://doi.org/10.1021/acssensors.0c01424>.
- [168] Zhang C, Zhou Y, Gu S, Wu Z, Wu W, Liu C, Wang K, Liu G, Li W, Lee PW. In silico prediction of hERG potassium channel blockage by chemical category approaches. *Toxicol Res*. 2016; 5(2):570. <https://doi.org/10.1039/c5tx00294j>.
- [169] Jordan MI, Mitchell TM. Machine learning: trends, perspectives, and prospects. *Science*. 2015;349(6245):255. <https://doi.org/10.1126/science.aaa8415>.
- [170] Moin A, Zhou A, Rahimi A, Menon A, Benatti S, Alexandrov G, Tamakloe S, Ting J, Yamamoto N, Khan Y. A wearable biosensing system with in-sensor adaptive machine learning for hand gesture recognition. *Nat Electron*. 2021;4(1):54. <https://doi.org/10.1038/s41928-020-00510-8>.
- [171] Chen J, Wang S, Wang K, Abiri P, Huang ZY, Yin J, Jabalera AM, Arianpour B, Roustaei M, Zhu E. Machine learning-directed electrical impedance tomography to predict metabolically vulnerable plaques. *Bioeng Transl Med*. 2023;9(1):616. <https://doi.org/10.1002/btm2.10616>.
- [172] Xiao X, Yin J, Shen S, Che Z, Wan X, Wang S, Chen J. Advances in solid-state fiber batteries for wearable bioelectronics. *Curr Opin Solid State Mater Sci*. 2022;26(6): 101042. <https://doi.org/10.1016/j.cossms.2022.101042>.
- [173] Xu J, Yin J, Fang Y, Xiao X, Zou Y, Wang S, Chen J. Deep learning assisted ternary electrification layered triboelectric membrane sensor for self-powered home security. *Nano Energy*. 2023;113:108524. <https://doi.org/10.1016/j.nanoen.2023.108524>.
- [174] Ma H, Qin H, Xiao X, Liu N, Wang S, Li J, Shen S, Dai S, Sun M, Li P. Robust hydrogel sensors for unsupervised learning enabled sign-to-verbal translation. *InfoMat*. 2023;5(7):e12419. <https://doi.org/10.1002/inf2.12419>.
- [175] Yu T, Fu Y, He J, Zhang J, Xianyu Y. Identification of antibiotic resistance in ESKAPE pathogens through plasmonic nanosensors and machine learning. *ACS Nano*. 2023;17(5): 4551. <https://doi.org/10.1021/acsnano.2c10584>.



- [176] Zhang K, Wang J, Liu T, Luo Y, Loh XJ, Chen X. Machine learning-reinforced noninvasive biosensors for healthcare. *Adv Healthc Mater.* 2021;10(17):2100734. <https://doi.org/10.1002/adhm.202100734>.
- [177] Tu J, Torrente-Rodríguez RM, Wang M, Gao W. The era of digital health: a review of portable and wearable affinity biosensors. *Adv Funct Mater.* 2020;30(29):1906713. <https://doi.org/10.1002/adfm.201906713>.
- [178] Ates HC, Nguyen PQ, Gonzalez-Macia L, Morales-Narváez E, Güder F, Collins JJ, Dincer C. End-to-end design of wearable sensors. *Nat Rev Mater.* 2022;7(11):887. <https://doi.org/10.1038/s41578-022-00460-x>.
- [179] Lee I, Probst D, Klonoff D, Sode K. Continuous glucose monitoring systems—Current status and future perspectives of the flagship technologies in biosensor research. *Biosens Bioelectron.* 2021;181:113054. <https://doi.org/10.1016/j.bios.2021.113054>.
- [180] Yao H, Shum AJ, Cowan M, Lähdesmäki I, Parviz BA. A contact lens with embedded sensor for monitoring tear glucose level. *Biosens Bioelectron.* 2011;26(7):3290. <https://doi.org/10.1016/j.bios.2010.12.042>.
- [181] Qu Y, Peng Q, Zhou Y, Manshahi F, Wang S, Wang K, Xie P, Qi X, Sun K. Fine-tunable  $\epsilon'$ -negative response derived from low-frequency plasma oscillation in graphene/polyaniline metacomposites. *Compos Commun.* 2023;44:101750. <https://doi.org/10.1016/j.coco.2023.101750>.
- [182] Kim J, Kim M, Lee MS, Kim K, Ji S, Kim T, Park J, Na K, Bae KH, Kyun KH. Wearable smart sensor systems integrated on soft contact lenses for wireless ocular diagnostics. *Nat Commun.* 2017;8(1):14997. <https://doi.org/10.1038/ncomms14997>.
- [183] Wang S, Nie Y, Zhu H, Xu Y, Cao S, Zhang J, Li Y, Wang J, Ning X, Kong D. Intrinsically stretchable electronics with ultrahigh deformability to monitor dynamically moving organs. *Sci Adv.* 2022;8(13):5511. <https://doi.org/10.1126/sciadv.abl5511>.
- [184] Ma X, Zhang M, Zhang J, Wang S, Cao S, Li Y, Hu G, Kong D. Highly permeable and ultrastretchable liquid metal micromesh for skin-attachable electronics. *ACS Mater Lett.* 2022; 4(4):634. <https://doi.org/10.1021/acsmaterialslett.1c00763>.
- [185] Zhu H, Wang S, Zhang M, Li T, Hu G, Kong D. Fully solution processed liquid metal features as highly conductive and ultrastretchable conductors. *npj Flex Electron.* 2021;5(1):25. <https://doi.org/10.1038/s41528-021-00123-x>.
- [186] Li Y, Wang S, Zhang J, Ma X, Cao S, Sun Y, Feng S, Fang T, Kong D. A highly stretchable and permeable liquid metal micromesh conductor by physical deposition for epidermal electronics. *ACS Appl Mater Interfaces.* 2022;14(11):13713. <https://doi.org/10.1021/acsami.1c25206>.
- [187] Gao W, Ota H, Kiriya D, Takei K, Javey A. Flexible electronics toward wearable sensing. *Acc Chem Res.* 2019;52(3): 523. <https://doi.org/10.1021/acs.accounts.8b00500>.
- [188] Hu G, Wang S, Yu J, Zhang J, Sun Y, Kong D. A facile and scalable patterning approach for ultrastretchable liquid metal features. *Lab Chip.* 2022;22(24):4933. <https://doi.org/10.1039/D2LC00872F>.
- [189] Wang J, Xu S, Zhang C, Yin A, Sun M, Yang H, Hu C, Liu H. Field effect transistor-based tactile sensors: from sensor configurations to advanced applications. *InfoMat.* 2023;5(1):2376. <https://doi.org/10.1002/inf2.12376>.

Springer Nature or its licensor (e.g. a society or other partner) holds exclusive rights to this article under a publishing agreement with the author(s) or other rightsholder(s); author self-archiving of the accepted manuscript version of this article is solely governed by the terms of such publishing agreement and applicable law.